CORE-MANTLE COUPLING

Paul H. Roberts[1], Jonathan M. Aurnou[2]
[1]Institute of Geophysics and Planetary Physics, University of California, Los Angeles, CA, USA
[2]Department of Earth and Space Sciences, University of California, Los Angeles, CA, USA

Definition, scope, and aims

The Earth is not a perfect timekeeper, and the spectrum of the variations in the mantle's angular velocity $\widehat{\mathbf{\Omega}}$ spans a wide range of frequencies. Of particular interest here are the comparatively large amplitude decadal and semi-decadal variations in which changes in length of day, P, of up to 2 ms occur. These would not be explained even if the global circulations of the atmosphere and oceans could be reversed. This is confirmed by a more detailed argument given in our recent review (Roberts and Aurnou, 2012), which will be referred to here as "RA12."

The origin of these length of day (LOD) variations must be sought in the Earth's core, and Figure 1 suggests that the task is not an easy one. Figure 1b shows dP/dt, derived by differentiating smoothed LOD data from the last half century, with atmospheric, oceanic, and tidal signals removed; semi-decadal time variations are clearly seen with a period τ_{LOD} of about 6 years (e.g., Abarca del Rio et al., 2000). Figure 1c shows the implied $\widehat{\Gamma}_z$ as a function of time t, where $\widehat{\Gamma}_z$ is the component parallel to the polar axis O_z of the torque $\widehat{\mathbf{\Gamma}}$ exerted by the core on the mantle. This shows that $\widehat{\Gamma}_z$ of nearly 10^{18} Nm is generated. We shall call this the "target torque" and seek its origin.

In addition, to the semi-decadal oscillations, larger variations seem to exist having longer periods, one of which is estimated to have a roughly 60 year period (e.g., Roberts et al., 2007). This time scale is reminiscent of the geomagnetic secular variation, and it is natural to seek

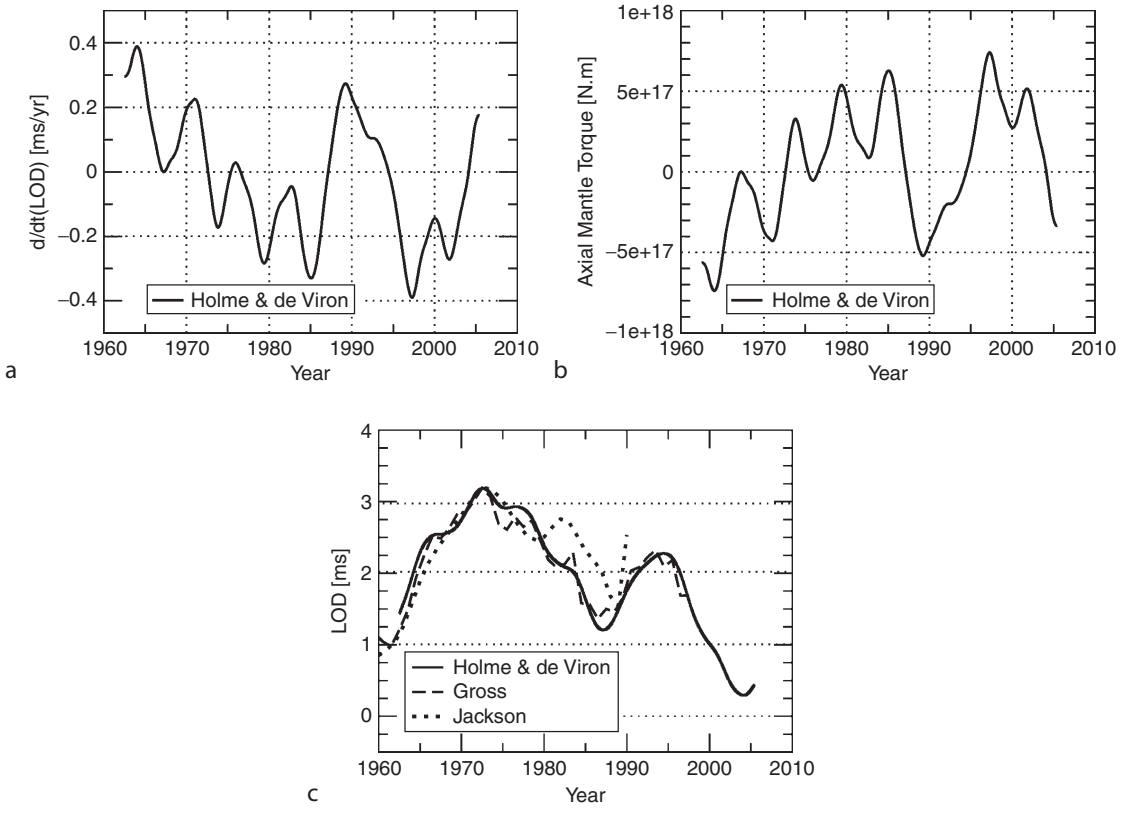

Core-Mantle Coupling, Figure 1 (**a**) LOD time series data from Holme and de Viron (2005) and Gross (2001) compared with LOD model from the "smooth" core flow inversion of Jackson (1997). The time series include the variation due to lunar tidal drag. (**b**) Temporal derivative, dP/dt, of the smoothed time series data of Holme and de Viron (2005), where P is the length of day. (**c**) The implied axial torque, $\widehat{\Gamma}_z = -(2\pi\widehat{C}/P^2)\mathrm{d}P/\mathrm{d}t$, on the mantle, where $\widehat{C}$ is the axial moment of inertia of the mantle. The LOD in panel (**a**) is arbitrary to within an additive constant, chosen here to obtain agreement at 1972.5 with Gross (2001).

a connection between them (e.g., Braginsky, 1970; Gillet et al., 2010). Figure 1c supports this quest. It shows the LOD data (Gross, 2001; Holme and de Viron, 2005) plotted against the estimated LOD variations inferred from the core flow models of Jackson (1997) that are based on inversion of geomagnetic secular variation data. The qualitative agreement implies that the variations in LOD are due to core-mantle angular momentum exchange associated with magnetohydrodynamic (MHD) processes in the core.

This review will focus on variations in LOD, i.e., changes in $\Omega_z(\approx \Omega)$. Precession and nutation of the Earth's axis, which describe variations in Ω_x and Ω_y, are also phenomena that cannot be satisfactorily explained without invoking core-mantle torques, but they are beyond the scope of this review. It will become clear that torques on the Solid Inner Core (SIC) are also of interest. Variables in the SIC will be distinguished by a tilde ($\widetilde{\ }$) and those in the mantle by a hat ($\widehat{\ }$). Except when making general statements, unadorned letters will refer to variables in the Fluid Outer Core (FOC).

The four coupling processes

The torque on the mantle about the geocenter O is

$$\widehat{\mathbf{\Gamma}} = \oint_{\widehat{\mathrm{S}}} \mathbf{r} \times \widehat{\mathbf{T}}\, \mathrm{dA}, \quad \text{where} \quad \widehat{T}_i = -\widehat{S}_{ij} n_j, \tag{1a,b}$$

sometimes called the "surface traction," is the stress associated with the normal and $\widehat{S}_{ij}$ is the total stress tensor; $\mathbf{r} = r\mathbf{1}_r$ is the radius vector from O, $r = |\mathbf{r}|$. The minus sign in Equation 1b arises because our unit normal, $\mathbf{n}$, to $\widehat{\mathrm{S}}$, the Core Mantle Boundary (CMB), points into the mantle. The axial torque, i.e., the component of $\widehat{\mathbf{\Gamma}}$ along the rotation axis Oz, is

$$\widehat{\Gamma}_z = -\oint_{\widehat{\mathrm{S}}} s\widehat{S}_{\phi n}\, \mathrm{dA}, \tag{1c}$$

where s is distance from the z-axis. For the torque on the SIC, we have similarly

$$\widetilde{\mathbf{\Gamma}} = \oint_{\widetilde{\mathrm{S}}} \mathbf{r} \times \widetilde{\mathbf{T}}\, \mathrm{dA}, \qquad \widetilde{T}_i = \widetilde{S}_{ij} n_j,$$
$$\widetilde{\Gamma}_z = \oint_{\widetilde{\mathrm{S}}} s\widetilde{S}_{\phi n}\, \mathrm{dA}; \tag{1d,e,f}$$

there is no minus sign in Equations 1e, f because our unit normal, $\mathbf{n}$, to the Inner Core Boundary (ICB) points out of the SIC.

Equation 1a tacitly assumes that the core alone exerts a torque on the mantle; sources of torque from outside the Earth are ignored, and therefore

$$\mathbf{\Gamma} + \widehat{\mathbf{\Gamma}} + \widetilde{\mathbf{\Gamma}} = \mathbf{0},$$
$$\mathbf{M} + \widehat{\mathbf{M}} + \widetilde{\mathbf{M}} = \text{constant}, \tag{1g,h}$$

where $\mathbf{\Gamma}$ is the torque on the FOC; $\mathbf{M}$, $\widehat{\mathbf{M}}$ and $\widetilde{\mathbf{M}}$ are the corresponding angular momenta. Equation 1g implies that, if one of the three torques changes, so do one or two of the others, in the opposite sense. The system is, in this respect, self-regulating. We shall treat the mantle and SIC as rigid bodies below.

Stress is exerted on the CMB in four ways: through viscosity, topography, gravity, and magnetic field, and there are correspondingly four parts to each of S_{ij}, $\mathbf{T}$ and $\mathbf{\Gamma}$, e.g., $\widehat{\mathbf{\Gamma}} = \widehat{\mathbf{\Gamma}}^V + \widehat{\mathbf{\Gamma}}^T + \widehat{\mathbf{\Gamma}}^G + \widehat{\mathbf{\Gamma}}^M$. The topographic and gravitational torques depend on the non-sphericity of $\widehat{\mathrm{S}}$ and $\widetilde{\mathrm{S}}$. For the others, negligible error is made by replacing the CMB and ICB by spheres, $\widehat{\mathrm{S}}_\bullet$ and $\widetilde{\mathrm{S}}_\bullet$, of radii r_o and r_i. The torques will be estimated below.

The viscous torque

Assuming uniform fluid density, ρ, and kinematic viscosity, ν, the part of the viscous stress tensor, $\widehat{S}^V_{ij}$, responsible for $\widehat{T}^V_i$ is $\rho\nu\nabla_j V_i$, i.e., $\widehat{\mathbf{T}}^V = -\rho\nu(\mathbf{n}\cdot\nabla)\mathbf{V} \approx -\rho\nu\partial_r\mathbf{V}$ so that, by Equations 1a, c,

$$\widehat{\mathbf{\Gamma}}^V = -\rho\nu \oint_{\widehat{\mathrm{S}}} \mathbf{r} \times \partial_r \mathbf{V}\, \mathrm{dA},$$
$$\widehat{\Gamma}^V_z = -\rho\nu \oint_{\widehat{\mathrm{S}}} s\partial_r V_\phi\, \mathrm{dA}. \tag{2a,b}$$

These torques involve only the radial gradient of the fluid velocity, $\mathbf{V}$. This tends to drag the mantle in the direction of the subsurface flow.

The viscosity of core fluid is hard to estimate. First principles calculations (de Wijs et al., 1998; Dobson et al., 2000; Vočadlo et al., 2000) suggest that ν at the CMB is within a factor of 3 of 10^{-6} m^2 s^{-1}. Suppose the viscous stress transfers momentum between the core and mantle over a length scale $d_\nu = E^{1/2} r_o \sim 0.2$ m, which is the thickness of the laminar Ekman boundary layer. Here

$$E = \nu/\Omega\mathcal{L}^2 \tag{2c}$$

is the Ekman number ($\approx 3 \times 10^{-15}$), which quantifies the ratio of the viscous and Coriolis forces; $\mathcal{L}$ is a characteristic scale of motion outside the boundary layer, for which we take $\mathcal{L} = r_o$. Assuming velocities of order $\mathcal{V} \approx 10^{-4}$ m s^{-1} (e.g., Jackson, 1997), the surface traction, $\widehat{T}^V \approx \rho\nu\mathcal{V}/d_\nu$, is about 10^{-5} N m^{-2}, implying that $\widehat{\Gamma}^V \approx 5 \times 10^{14}$ Nm.

In a highly turbulent medium such as the FOC, small scale motions transport macroscale quantities, such as angular momentum, far more effectively than molecular diffusion. When these scales are too small to be resolved by numerical computations, they are termed "sub-grid scales." Their effect must then be included in some other way. Appeal is often made to an analogy with molecular diffusion. Molecular transport depends on the molecular mean-free-path, ℓ, and the rms molecular speed, u. Simple

dynamical arguments show that the molecular diffusivity, ν, for momentum is of order $u\ell$. The analogy pictures small scale eddies replacing molecules as the transporters of macroscale momentum. The correlation length, $l_{\rm cor}$, of the turbulence replaces ℓ and the rms turbulent velocity, υ, replaces u. The transport of macroscale momentum is then governed by a kinematic "turbulent viscosity" $\nu_T \approx \upsilon l_{\rm cor}$, which greatly exceeds ν. We use $\upsilon = 10^{-4}$ m s^{-1} for the velocity scale. The length scale is harder to estimate. Here we take $l_{\rm cor} \sim E^{1/3} r_o \approx 100$ m, which is based upon the characteristic length scale for finite amplitude rapidly rotating convection (e.g., Stellmach and Hansen, 2004; Sprague et al., 2006). This gives $\nu_T \approx 10^{-2}$ m^2 s^{-1}. Though it is strictly inconsistent to use υ and $l_{\rm cor}$ when estimating the shear on the resolved scales, an upper bound on the turbulent traction follows from doing so: $\widehat{T}^V \approx \rho \nu_T \upsilon / l_{\rm cor} \approx \rho (\upsilon l_{\rm cor}) \upsilon / l_{\rm cor} \approx 10^{-4}$ N m^{-2}, implying $\widehat{\Gamma}^V_z \approx 5 \times 10^{15}$ Nm.

This may overestimate $\widehat{\Gamma}^V_z$. A stable layer may exist at the top of the FOC; see, e.g., Loper (2007), Buffett (2010). Braginsky (1999) pointed out that the light material released during the freezing of the SIC may preferentially congregate near the ICB, and that this may answer unresolved questions about the geomagnetic secular variation (Braginsky, 1984). Turbulent motions in a buoyantly stable layer tend to be damped preferentially in the direction of stratification, and this reduces the macroscale momentum transport across the layer (e.g., Gargett, 1984; Davidson, 2004). Waves in such a layer may increase what ν alone can do in transporting macroscale momentum (e.g., Rogers and Glatzmaier, 2006). But it is doubtful if they can transport it as effectively as ν_T for fully convective turbulence far from boundaries.

Though these and similar arguments lack rigor, the above estimates of $\widehat{\Gamma}^V$ are less than the target torque, but not vastly so (cf. Kuang and Bloxham, 1997; Brito et al., 2004; Deleplace and Cardin, 2006; Buffett and Christensen, 2007).

The topographic torque

The likelihood that there are inverted mountains and valleys on the CMB, and that these might create topographic torques large enough to explain the observed changes in LOD, was first suggested by Hide (1969). These irregularities are often collectively called "bumps," and their study was jokingly christened "geophrenology" by the late Keith Runcorn. Hide's idea generated much interest and literature, e.g., Anufriev and Braginsky (1975; 1977a; b), Jault and Le Mouël (1989), Kuang and Bloxham (1993, 1997), Buffett (1998) and Kuang and Chao (2001). Seismic studies infer the bump height, $\mathcal{H}$, is of order 1 km (e.g., Tanaka, 2010). See *Earth's Structure, Lower Mantle*.

Topographic coupling between the FOC and its boundaries depends on deviations from sphericity in the shapes of the CMB and ICB. The fluid pressure, p, creates surface tractions, $\widehat{\mathbf{T}}^T = p\mathbf{n}$ and $\widetilde{\mathbf{T}}^T = -p\mathbf{n}$, that are not purely radial. The resulting topographic torques on the CMB and ICB are

$$\begin{aligned} \widehat{\mathbf{\Gamma}}^T &= \oint_{\widehat{\rm S}} p\mathbf{r} \times \mathbf{n}\, {\rm dA}, \\ \widetilde{\mathbf{\Gamma}}^T &= -\oint_{\widetilde{\rm S}} p\mathbf{r} \times \mathbf{n}\, {\rm dA}. \end{aligned} \tag{3a,b}$$

Equal but opposite torques act on the FOC, so that (cf. Equation 1g)

$$\mathbf{\Gamma}^T = -\widehat{\mathbf{\Gamma}}^T - \widetilde{\mathbf{\Gamma}}^T = -\int_{\rm V} \mathbf{r} \times \boldsymbol{\nabla} p\, {\rm dV}. \tag{3c}$$

We define the CMB and ICB by

$$r = r_o + \widehat{h}(\theta, \phi), \quad r = r_i + \widetilde{h}(\theta, \phi), \tag{4a,b}$$

where $(r,\ \theta,\ \phi)$ are spherical coordinates. Equations 3a, b can be simplified if it is assumed that $\left|\widehat{h}\right|/r_o \ll 1, \left|\widetilde{h}\right|/r_i \ll 1, \left|\boldsymbol{\nabla}\widehat{h}\right| \ll 1$ and $\left|\boldsymbol{\nabla}\widetilde{h}\right| \ll 1$; see RA12. The projection of Equations 3a, b onto the spheres $\widehat{\rm S}_\bullet$ and $\widetilde{\rm S}_\bullet$ are then

$$\begin{aligned} \widehat{\mathbf{\Gamma}}^T &= \oint_{\widehat{\rm S}_\bullet} \widehat{h}\mathbf{r} \times \boldsymbol{\nabla} p\, {\rm dA}_\bullet, \\ \widetilde{\mathbf{\Gamma}}^T &= -\oint_{\widetilde{\rm S}_\bullet} \widetilde{h}\mathbf{r} \times \boldsymbol{\nabla} p\, {\rm dA}_\bullet. \end{aligned} \tag{4c,d}$$

The torques $\widehat{\mathbf{\Gamma}}^T$ and $\widetilde{\mathbf{\Gamma}}^T$ obviously depend on variations in p in the FOC, and we consider next the causes and magnitudes of these. This necessitates a considerable digression. The first step is to develop a reference state.

Convection mixes the FOC so well that, except in thin boundary layers at the CMB and ICB, it is chemically and thermodynamically homogeneous. It is therefore isentropic, i.e., its specific entropy, S, is uniform. The core is an unknown mixture of all elements, but the basics can be understood by assuming that it is a binary alloy of Fe and a lighter element, X, whose mass fraction is X. It is usually supposed that X is mostly Si or S, but it is unnecessary to be specific here. Except in boundary layers,

$$\begin{aligned} S &= S_a = \text{Constant}, \\ X &= X_a = \text{Constant, in the FOC}, \end{aligned} \tag{5a,b}$$

where the suffix $_a$ stands for "adiabatic".

Although fast enough to mix the core thoroughly, core flows are slow compared with the speed of sound, u_s ($\approx 10^4$ m s^{-1}). The primary dynamical balance is therefore hydrostatic and, allowing for centrifugal forces, it is governed by

$$\begin{aligned} \boldsymbol{\nabla} p_a &= \rho_a (\mathbf{g}_a - \mathbf{\Omega} \times (\mathbf{\Omega} \times \mathbf{r})) \\ &= \rho_a \left(\mathbf{g}_a + \frac{1}{2} \nabla (\mathbf{\Omega} \times \mathbf{r})^2 \right), \end{aligned} \tag{5c}$$

where $\mathbf{\Omega} = \Omega \mathbf{1}_z$ is the angular velocity of the Earth and $\mathbf{g}$ is the gravitational acceleration. Newtonian gravitation theory requires that

$$\boldsymbol{\nabla} \times \mathbf{g} = \mathbf{0}, \quad \boldsymbol{\nabla} \cdot \mathbf{g} = -4\pi G\rho, \tag{5d,e}$$

where G is the constant of gravitation. It follows that

$$\boldsymbol{\nabla} p_a = \rho_a \mathbf{g}_e = -\rho_a \boldsymbol{\nabla} \Phi_e, \quad \text{where} \quad \mathbf{g}_e = -\boldsymbol{\nabla}\Phi_e \tag{5f,g}$$

is the effective gravitational field and $\Phi_e = \Phi_a - \frac{1}{2}(\mathbf{\Omega} \times \mathbf{r})^2$ is the "effective gravitational potential." Equation 5d shows that p_a, ρ_a, . . . are constant on equipotential surfaces:

$$p_a = p(\Phi_e, S_a, X_a),$$
$$\rho_a = \rho(\Phi_e, S_a, X_a) = -\partial p(\Phi_e, S_a, X_a)/\partial \Phi_e, \ldots \tag{5h,i}$$

The effect of the centrifugal forces is quantified by $\varepsilon_\Omega = \Omega^2 r/g$. This is small, varying from 1.7×10^{-3} at the CMB to 1.5×10^{-3} at the ICB. The deviation of the equipotential surfaces from spheres is therefore small, as are deviations caused by the gravitational field produced by density anomalies in the mantle and SIC, quantified below. It is therefore helpful to refer to departures from a "reference state" that is spherically symmetric: $\Phi = \Phi^s(r)$, $p = p^s(r)$, $\rho = p^s(r)$, $T = T^s(r)$, etc., where T is temperature. There are large departures from adiabaticity in boundary layers and smaller departures throughout the FOC that are of two main types:

(a) *Deviations from Φ^s due to rotation and density anomalies in the mantle and SIC.* These will be denoted by a prime, e.g., $p'_a = p_a - p^s$. Rotation produces the larger deviation but, as will be seen below, this is less relevant to LOD variations than the anomaly created by the mantle, which in the FOC is dominantly

$$\Phi'_a = A'(r/r_o)^2 \sin^2\theta \cos\ 2\phi, \quad (A' > 0) \tag{6}$$

Wahr and deVries (1989), Forte et al. (1994). The value of the constant A' is about 1,300 $m^2\ s^{-2}$, according to Defraigne et al. (1996) and about 2,300 $m^2\ s^{-2}$ according to Forte et al. (1994); our compromise will be A' =1,800 $m^2\ s^{-2}$. By Equation 5i, $p'_a \approx -\rho^s_a \Phi'_a$. Therefore $\varepsilon_a = p'_a/p^s_a$ is 10^{-4} on the CMB equator and 10^{-5} at the ICB equator.

(b) *Deviations created by convection.* We use the notation

$$\rho = \rho_a + \rho_c, \tag{7a}$$

and similarly for other variables. The Earth radiates energy into space at a rate estimated to exceed 43 TW (e.g., §4.1.5 of Schubert et al., 2001). We take an extreme position by supposing the entire 43 TW emerges from the core. The outward heat flux in the FOC is the sum of the convective heat flux q_c and the adiabatic heat flux $q_a = -KdT^s/dr$, where K is thermal conductivity. Though the latter may be as much as 5 TW, we ignore it. Then q_c = 0.28 W m^{-2} at the CMB. We take

$$q_c = \rho c_p \overline{T_c V_r}, \tag{7b}$$

where c_p (≈800 J kg^{-1} K^{-1}) is the specific heat at constant pressure, p. The overline denotes a horizontal average over the flow, which is undoubtedly highly turbulent. For $V_r = 10^{-4}$ m s^{-1}, it follows that $T_c = 3.5 \times 10^{-4}$ K. As $T_a \approx 4,000$ K (e.g., Kawai and Tsuchiya, 2009), $\varepsilon_c = T_c/T_a$ is less than 10^{-7}, which is 3–4 orders of magnitude smaller than ε_a. Even this is an overestimate; it has never been suggested that Q_c is larger than 15 TW. The smallness of ε_Ω, ε_a, and ε_c means that all these effects can be treated as perturbations of the reference state.

As $p'_a(r,\ \theta,\ \phi) \gg p_c(r,\ \theta,\ \phi)$, it is sensible to consider first the effect of p'_a by introducing the "adiabatic topographic torques" on the mantle, ICB, and FOC:

$$\widehat{\mathbf{\Gamma}}^T_a = \oint_{\widehat{S}} p_a\, \mathbf{r} \times \mathbf{n}\, dA,$$
$$\widetilde{\mathbf{\Gamma}}^T_a = -\oint_{\widetilde{S}} p_a\, \mathbf{r} \times \mathbf{n}\, dA, \tag{8a,b,c}$$
$$\mathbf{\Gamma}^T_a = -\int_V \mathbf{r} \times \boldsymbol{\nabla} p_a\, dV.$$

If the CMB (ICB) were an equipotential or if it were spherical, $\widehat{\mathbf{\Gamma}}^T_a \left(\widetilde{\mathbf{\Gamma}}^T_a\right)$ would vanish according to Equation 8a, b, but generally these torques are nonzero. They can be evaluated only if $\widehat{p}$ ($\widetilde{p}$) is known on the CMB (ICB). It will be shown in the next section that $\widehat{\mathbf{\Gamma}}^T_a$ and $\widetilde{\mathbf{\Gamma}}^T_a$ are intimately related to what we shall call "adiabatic gravitational torques." We therefore postpone further discussion and estimation of adiabatic topographic torques.

Consider the torque $\widehat{\mathbf{\Gamma}}^T_c$ associated with the convective motions in the FOC:

$$\widehat{\mathbf{\Gamma}}^T_c = \oint_{\widehat{S}_\bullet} \widehat{h}\mathbf{r} \times \boldsymbol{\nabla} p_c\, dA_\bullet,$$
$$\widehat{\Gamma}^T_{c,z} = \oint_{\widehat{S}_\bullet} \widehat{h}\partial_\phi p_c\, dA_\bullet. \tag{9a,b}$$

Reasons will be given in the section on the "Magnetic Torque" why core flow may be well described by the magnetostrophic approximation Equation 20a, and why, deep in the core, Coriolis and Lorentz forces are comparable, implying a magnetic field strength $\mathcal{B}$ there of about 2 mT, or about four times greater than the typical field strength $\mathcal{B}_o$ on the CMB. The Lorentz force is therefore 16 times less on the CMB than in the bulk of the core. Also, as g_ϕ, is small, $\partial_\phi p_c \approx -2\Omega\rho_0 r_o V_\theta \cos\theta \sin\theta$ should be a good approximation to the ϕ-component of Equation 20a on the CMB. Therefore (Hide et al., 1993)

$$\widehat{\Gamma}^T_{c,z} = -2\Omega\rho_0 r_o \oint_{\widehat{\mathrm{S}}_\bullet} \widehat{h}(\theta,\phi) V_\theta(r_o,\theta,\phi)\cos\theta\sin\theta\,\mathrm{dA}_\bullet. \tag{9c}$$

In principle, $\widehat{\Gamma}^T_{c,z}$ can be estimated by extracting $\widehat{h}$ from seismological analysis, and by using the V_θ (r_o, θ, ϕ) inferred from the core surface motion. In practice, this is difficult and has generated controversy. Equation 9c suggests that

$$\widehat{\Gamma}^T_{c,z} = \mathrm{O}\left(2\Omega\rho\mathcal{V}\mathcal{H}r_o^3\right), \tag{9d}$$

which is 10^{18} Nm for a bump height of $\mathcal{H}$ = 100 m. Such a bump height is well within the bounds set by recent seismic investigations (e.g., Tanaka, 2010). Equation 9b indicates, however, that Equation 9d may be a serious overestimate because p_c is a single-valued function and $\partial_\phi\, p_c$ is as often positive as negative in the integrand of Equation 9b. Though $\pm 2\Omega\rho\mathcal{V}r_o$ is a reasonable estimate of $\partial_\phi\, p_c$ at most points on the CMB, considerable cancellation is likely when evaluating the integral in Equation 9b. There is even an outside chance that the cancellation might be complete; see Anufriev and Braginsky (1978b).

Reliable estimation of the convective topographic torque must probably await careful experiments and allied theory. No argument has so far convincingly demonstrated that topography can create torques of the target magnitude of 10^{18} Nm but, equally, none have shown that it cannot.

The gravitational torque

The gravitational torque on a body V of density $\rho(\mathbf{x})$ in a gravitational field $\mathbf{g}(\mathbf{x})$ is

$$\mathbf{\Gamma}^G = \int_{\mathrm{V}} \rho\,\mathbf{r}\times\mathbf{g}\,\mathrm{dV}. \tag{10a}$$

This volume integral can be usefully transformed into a surface integral by drawing on the analogy between the theories governing Newtonian gravitation and electrostatics, the only difference between these theories being one of sign: like charges repel but all bodies attract gravitationally. It can be shown that

$$\rho g_i = \nabla_j S^G_{ij}, \quad \text{where} \quad S^G_{ij} = -\frac{1}{4\pi G}\left(g_i g_j - \frac{1}{2}g^2\delta_{ij}\right) \tag{10b,c}$$

is the gravitational stress tensor, the gravitational pressure $-g^2/8\pi G$ being also the gravitational energy density. Equations 10b, c enable Equation 10a to be written as a surface integral:

$$\mathbf{\Gamma}^G = -\frac{1}{4\pi G}\oint_{\mathrm{S}} \mathbf{r}\times\left[(\mathbf{n}\cdot\mathbf{g})\mathbf{g} - \frac{1}{2}g^2\mathbf{n}\right]\mathrm{dA}, \tag{10d}$$

where $\mathbf{n}$ points out of V. See RA12 and Appendix B of Braginsky and Roberts (1995) for derivations of these results. When they are applied below, $\mathbf{n}$ on the CMB and SIC will, as previously defined, be oriented approximately parallel to $\mathbf{r}$.

By Equation 10a, the gravitational torque on the FOC due to the mantle and SIC is

$$\mathbf{\Gamma}^G = \int_{\mathrm{V}} (\rho_a+\rho_c)\mathbf{r}\times(\mathbf{g}_a+\mathbf{g}_c)\mathrm{dV} = \mathbf{\Gamma}^G_a + \mathbf{\Gamma}^G_c, \tag{11a}$$

where $\mathbf{\Gamma}^G_a$ and $\mathbf{\Gamma}^G_c$ are the adiabatic and convective parts of $\mathbf{\Gamma}^G$:

$$\mathbf{\Gamma}^G_a = \int_{\mathrm{V}} \rho_a\mathbf{r}\times\mathbf{g}_a\,\mathrm{dV}, \qquad \mathbf{\Gamma}^G_c = \int_{\mathrm{V}} \mathbf{r}\times(\rho_c\mathbf{g}_a + \rho_a\mathbf{g}_c + \rho_c\mathbf{g}_c)\mathrm{dV}. \tag{11b,c}$$

It was pointed out earlier that $\rho_c = \mathrm{O}(10^{-4}\rho'_a)$, $g_c = \mathrm{O}(10^{-4}g'_a)$, etc. Apparently therefore $\Gamma^G_c = \mathrm{O}(10^{-4}\Gamma^G_a)$, making it sensible to focus first on the adiabatic torque.

Consistent with hydrostatic balance in the FOC (see Equation 5f), Equations 8c and 11b, give

$$\mathbf{\Gamma}^{G+T}_a = \mathbf{\Gamma}^G_a + \mathbf{\Gamma}^T_a = \int_{\mathrm{V}} \mathbf{r}\times(\rho_a g_a - \boldsymbol{\nabla}p_a)\mathrm{dV} = \mathbf{0}. \tag{12a}$$

By Equations 8a, b and 10d and the continuity of $\mathbf{g}$ and p, we also have

$$\widehat{\mathbf{\Gamma}}^{G+T}_a = \oint_{\widehat{\mathrm{S}}} \mathbf{r}\times\left\{p_a\mathbf{n} + (4\pi G)^{-1}\left[(\mathbf{n}\cdot\mathbf{g}_a)g_a - \frac{1}{2}g_a^2\mathbf{n}\right]\right\}\mathrm{dA}, \tag{12b}$$

$$\widetilde{\mathbf{\Gamma}}^{G+T}_a = -\oint_{\widetilde{\mathrm{S}}} \mathbf{r}\times\left\{p_a\mathbf{n} + (4\pi G)^{-1}\left[(\mathbf{n}\cdot\mathbf{g}_a)g_a - \frac{1}{2}g_a^2\mathbf{n}\right]\right\}\mathrm{dA}, \tag{12c}$$

from which, in agreement with Equation 12a,

$$\widehat{\mathbf{\Gamma}}^{G+T}_a + \widetilde{\mathbf{\Gamma}}^{G+T}_a = \mathbf{0}. \tag{12d}$$

If the torques $\widehat{\mathbf{\Gamma}}^{G+T}_a$ and $\widetilde{\mathbf{\Gamma}}^{G+T}_a$ are nonzero, $\widehat{\mathbf{\Omega}}$ and $\widetilde{\mathbf{\Omega}}$ evolve. The consequent change in the relative orientation of the mantle and SIC modifies $\mathbf{g}_a$ and p_a in Equation 12b, c so that the system evolves toward a configuration of minimum energy E. In this configuration

$$\widehat{\mathbf{\Gamma}}^{G+T}_a = \mathbf{0}, \qquad \widetilde{\mathbf{\Gamma}}^{G+T}_a = \mathbf{0}. \tag{13a,b}$$

If this minimum energy, torque-free state is perturbed, the restoring GT-torques (as we shall call them) set up a "gravitational oscillation" of the SIC relative to the mantle.

To give a simple example, suppose that the gravitational anomaly defined by Equation 6 is created by sources entirely within the mantle, the CMB having no

bumps, so that $\widehat{\Gamma}^{G+T}_{a,z} = \widehat{\Gamma}^{G}_{a,z}$. Similarly, suppose the SIC is spherical but has internal sources that above the ICB produce the gravitational anomaly

$$\Phi''_a = A''(r_i/r)^3 \sin^2\theta \cos 2(\phi - \varphi), \quad (A'' > 0), \tag{14a}$$

where φ is the angular displacement of the system from the stable state, $\varphi = 0$, in which Equations 13a, b hold. Equations 12b, c show that

$$\widehat{\Gamma}^{G}_{a,z} = -\widetilde{\Gamma}^{G}_{a,z} = \Gamma^{G}_{0} \sin 2\varphi, \quad \text{where} \quad \Gamma^{G}_{0} = 8A'A''r_i^3/3Gr_o^2 (> 0). \tag{14b,c}$$

These torques vanish for the stable minimum energy states $\varphi = 0, \pi$ (and also for the unstable $\varphi = \pm\frac{1}{2}\pi$). Small departures from a stable state satisfy

$$\widehat{C}d_t^2\widehat{\varphi} = 2\Gamma^{G}_{0}(\widetilde{\varphi} - \widehat{\varphi}), \quad \widetilde{C}d_t^2\widetilde{\varphi} = 2\Gamma^{G}_{0}(\widetilde{\varphi} - \widehat{\varphi}), \tag{14d,e}$$

where $\widehat{C}$ (= 7.12 × 10^{37} kg m^2) and $\widetilde{C}$(= 5.86 × 10^{34} kg m^2) are the polar moments of inertia of mantle and SIC, respectively. The frequency, ω^G, of the oscillation is

$$\omega^G = [2(\widehat{C} + \widetilde{C})\Gamma^{G}_{0}/\widehat{C}\widetilde{C}]^{1/2} \approx [2\Gamma^{G}_{0}/\widetilde{C}]^{1/2}. \tag{14f}$$

Although an anomaly of the form of Equation 14a could be produced by density variations within the SIC, it is more plausibly created by SIC topography for the following reasons. It is generally believed that the SIC is the result of freezing of the FOC, an ongoing process even today (Jacobs, 1953). An alloy generally changes its composition when it changes phase. The rather large density jump at the ICB, $\widetilde{\Delta} = \widetilde{\rho}(r_i) - \rho(r_i) \approx 600\,\mathrm{kg\,m^{-3}}$, is hard to attribute to contraction on freezing but can be readily explained as a small reduction in X on freezing. Phase equilibrium at the ICB implies $T^s_a(\Phi_a, S_a, X_a) = T_m(p_a, X_a)$, where T_m is the melting temperature. This implies that the ICB is an equipotential surface. Since $\Phi = \Phi^s_a(r) + \Phi'_a(r,\theta,\phi)$ where $|\Phi'_a/\Phi^s_a| \ll 1$, Taylor expansion, using Equation 4b, shows that $\Phi^s_a(r_i) + \widetilde{g}\widetilde{h}(\theta,\phi) + \Phi'_a(r_i,\theta,\phi)$ is approximately constant, where $\widetilde{g} = -g^s_{a,r}(r_i) = \partial_r\Phi^s_a(r_i)(> 0)$ is gravity at the ICB. It follows that

$$\widetilde{h} = -\Phi'_a(r_i,\theta,\phi)/\widetilde{g} = \widetilde{\varepsilon}\,\sin^2\theta\cos 2\phi, \quad \widetilde{\varepsilon} = -A'(r_i/r_o)^2/\widetilde{g}. \tag{14g,h}$$

This shows how the gravitational anomaly in the mantle imposes its $n = m = 2$ preference on the SIC. It makes the otherwise ad hoc assumption of Equation 14a seem perfectly reasonable. The condition that $\widetilde{h}$ creates Equation 14a, for $\varphi = 0$ and $r - r_i \ll \widetilde{h}$ is

$$A''/A' = 4\pi G r_i^3\widetilde{\Delta}/5r_o^2\widetilde{g} \approx 0.0034. \tag{14i}$$

The maximum bump height on the ICB is $|\widetilde{\varepsilon}| \approx 50$ m. Nonzero φ corresponds to a rotated SIC. Such a rotation is to be expected; core turbulence continually subjects the SIC to (topographic) torques that continuously change its orientation. Two relaxation processes act to restore the ICB to its equipotential: (i) flow within the SIC, (ii) new freezing/melting on the ICB. If either were instantaneous, there would be no torque between the mantle and SIC, but both appear to act on much longer time scales than core turbulence, so that SIC topography is almost "frozen" to the SIC as it turns.

Concerning (i), the viscosity of the SIC is plausibly much less than the viscosity of the mantle. According to Schubert et al. (2001) $\widehat{\nu} \approx 5 \times 10^{19}\mathrm{m^2\,s^{-1}}$ in the deep mantle but, according to Mound and Buffett (2006), $\widetilde{\nu} \gtrsim 10^{13}\mathrm{m^2\,s^{-1}}$. Whereas mantle anomalies are essentially "frozen in," slow motions within the SIC created by stresses exerted by the FOC on the ICB can gradually restore equilibrium (Yoshida et al., 1996; Buffett, 1997). Concerning (ii), the thermodynamic disequilibrium created by the misalignment of the ICB from its equipotential surface is slowly removed by new freezing of the FOC or new melting of the SIC. This processes has not been fully explored (but see Fearn et al., 1981; Morse, 1986). The possible significance of melting/freezing processes on SIC structure has been recently investigated by Alboussière et al. (2010) and Monnereau et al. (2010).

Interest in gravitational torques and oscillations was sparked by Buffett (1996). We follow him but by a different method, making use of Equations 14c, i:

$$\Gamma^{G}_{0} = 32\pi r_i^6\widetilde{\Delta}A'^2/15r_o^4\widetilde{g} \approx 6.7 \times 10^{19}\,\mathrm{Nm} \tag{15a}$$

By Equation 14f, the frequency of the oscillation is $\omega^G \approx 4.8 \times 10^{-8}\,\mathrm{s^{-1}}$, with a period of

$$\tau^G = 2\pi/\omega^G \approx 4.1\,\text{years}. \tag{15b}$$

According to Buffett et al. (2009), gravitational oscillations are mainly responsible for the LOD variations shown in Figure 1. Mound and Buffett (2006) obtain $\Gamma^{G}_{0} \approx 1.5 \times 10^{20}$ Nm.

Equations 14d, e imply, for some t_0,

$$\widehat{\Omega} = \widehat{\Omega}_0 + d_t\widehat{\phi} = \widehat{\Omega}_0 + (2\Gamma^{G}_{0}/\widehat{C}\omega^G)(\widetilde{\phi} - \widehat{\phi})_{\max}\sin\omega^G(t - t_0). \tag{15c}$$

The amplitude of the gravitational oscillation is therefore related to that of the variation, ΔP, in LOD by

$$\left(\widetilde{\phi} - \widehat{\phi}\right)_{\max} = \pi\widehat{C}\omega^G\Delta P/\Gamma^{G}_{0}P_0^2 \approx 1.2^\circ, \tag{15d}$$

for ΔP = 1 ms. This gives a maximum angular velocity difference of $\omega^G\left(\widetilde{\phi} - \widehat{\phi}\right)_{\max} \approx 2^\circ\,\mathrm{year^{-1}}$. Furthermore the peak-to-peak variation in the radial gravitational acceleration at the Earth's surface, $r = r_E$, is

$$\Delta g_r''(r_E) = \frac{12A''}{r_i}\left(\frac{r_i}{r_E}\right)^4 (\widehat{\phi} - \widetilde{\phi})^2_{\max} \simeq 4\,\text{nGal}. \quad (15e)$$

This value is too small by roughly a factor of 5 to be detectable by the GRACE satellite system (e.g., Wahr et al., 2006).

One limitation of this analysis is the neglect of electromagnetic stresses at the boundaries when they are in motion relative to the core fluid. It has been implicitly assumed that the SIC is completely decoupled from the fluid within the tangent cylinder (TC), the imaginary cylinder that touches the ICB at its equator. This is particularly significant because the fluid dynamics inside and outside the TC are quite dissimilar. See Hide and James (1983), Heimpel and Aurnou (2007), and the next section. Because the SIC is as good an electrical conductor as the FOC (or better), it may be tightly coupled magnetically to $\mathcal{C}^N$ and $\mathcal{C}^S$, as suggested by Braginsky (1970); see the next section. To examine the effect of this coupling, we make the extreme assumption that all the fluid in the TC is completely locked to the SIC. Because the mantle is a poor electrical conductor, this fluid is not well coupled to the mantle, so that the entire fluid column within the TC can co-rotate about O_z almost freely with the SIC. This suggests that, instead of Equations 1g, h, a more useful division of the total angular momentum of the Earth might be based on

$$\widehat{\mathbf{\Gamma}} + \mathbf{\Gamma}^{\text{TC}} + \mathbf{\Gamma}^{\text{XTC}} = \mathbf{0}, \qquad \widehat{\mathbf{M}} + \mathbf{M}^{\text{TC}} + \mathbf{M}^{\text{XTC}} = \text{constant}, \quad (16a,b)$$

where $^{\text{TC}}$ refers to the TC and SIC locked together, and $^{\text{XTC}}$ refers to the part of the FOC exterior to the TC. The moment of inertia of the fluid within the TC is 2.12×10^{35} kg m^2 which, when added to $\widetilde{C}$, gives $C^{\text{TC}} = 2.71 \times 10^{35}$ kg m^2. Using this instead of $\widetilde{C}$ in Equation 14f, τ^{G} is lengthened from 4.1 years to

$$\tau^G_{\text{TC}} = 2\pi/\omega^G_{\text{TC}} \approx 8.9 \text{ years}, \quad \text{where } \omega^G_{\text{TC}} = [2(\widehat{C} + C^{\text{TC}})\Gamma^G_0/\widehat{C}C^{\text{TC}}]^{1/2}. \quad (16c,d)$$

See also Mound and Buffett (2006).

Even though ρ_c/ρ_a, p_c/p_a, etc., are of order 10^{-4}, this does not mean that $\Gamma_c^{G+T}/\Gamma_a^{G+T}$ is as small as that. In fact, Equation 13a shows that $\mathbf{\Gamma}_a^{G+T} = \mathbf{0}$ in the minimum energy state. The adiabatic GT-torques dominate the convective torques only if φ is sufficiently large. Stated another way, a convective torque can be nullified by a small departure from the minimum energy state. Earlier, the torque on the SIC created by core turbulence was held responsible for causing φ to deviate from zero. This torque is essentially (magneto-)convective, and is nullified by the GT-torque for a tiny change in φ. Another way of estimating how tiny this φ is equates the magnitudes of the GT-torque, taken as $1.3 \times 10^{20}\,\varphi$ Nm (see Equations 14b, c and 15d), and the convective torque, taken to have its target value of 10^{18} Nm. This gives $\varphi \approx 0.5°$. Within this angle, the mantle and SIC are gravitationally locked together, over short time scales compared with those of the relaxation processes in the SIC described above. See Buffett and Glatzmaier (2000).

The magnetic torque

This section assumes that readers are familiar with pre-Maxwell EM theory and the fundamentals of MHD, including the frozen flux theorem and Alfvén waves. Davidson (2001) contains the necessary background.

It may be useful to remind readers that the magnetic torque about O on a body V carrying a current of density $\mathbf{J}$ is the integrated moment of the Lorentz force, $\mathbf{J} \times \mathbf{B}$:

$$\mathbf{\Gamma}^M = \int_{\text{V}} \mathbf{r} \times (\mathbf{J} \times \mathbf{B})\,\text{dV} = \int_{\text{V}} r[B_r\mathbf{J} - J_r\mathbf{B}]\,\text{dV}. \quad (17a)$$

The Lorentz force can be expressed as a divergence:

$$(\mathbf{J} \times \mathbf{B})_i = \nabla_j S^M_{ij}, \quad \text{where } S^M_{ij} = \mu_0^{-1}\left(B_iB_j - \frac{1}{2}B^2\delta_{ij}\right) \quad (17b,c)$$

is the magnetic stress tensor. An alternative form of Equation 17a is therefore

$$\mathbf{\Gamma}^M = \mu_0^{-1}\oint_{\text{S}} \mathbf{r} \times \left[(\mathbf{n}\cdot\mathbf{B})\mathbf{B} - \frac{1}{2}B^2\mathbf{n}\right]\text{dA}, \quad (17d)$$

where the unit normal $\mathbf{n}$ to S points out of V. Therefore

$$\widehat{\Gamma}^M_z = -\mu_0^{-1}\oint_{\widehat{\text{S}}} s\widehat{B}_r\widehat{B}_\phi\,\text{dA}, \quad \widetilde{\Gamma}^M_z = \mu_0^{-1}\oint_{\widetilde{\text{S}}} s\widetilde{B}_r\widetilde{B}_\phi\,\text{dA}. \quad (17e,f)$$

These results can be used as they stand to assess the magnetic coupling between the inferred core surface flow and the mantle. See Stix and Roberts (1984), Love and Bloxham (1994), Holme (1998). Here, however, we are more interested in forging a link between the observed changes in LOD and torsional waves. To explain what the latter are, it is necessary to consider some dynamical issues.

Most studies of core MHD are based on the Boussinesq approximation; see, e.g., Braginsky and Roberts (2007). This assumes constant density, $\rho_0 (\approx 10^4 \text{kg m}^{-3})$, and expresses conservation of mass and momentum as

$$\nabla\cdot\mathbf{V} = 0, \quad \partial_t\mathbf{V} + \mathbf{V}\cdot\nabla\mathbf{V} + 2\Omega\times\mathbf{V} = -\nabla(p_c/\rho_0) + \mathcal{C}\mathbf{g}_e + \mathbf{J}\times\mathbf{B}/\rho_0 + \nu_T\nabla^2\mathbf{V}. \quad (18a,b)$$

The accelerations in Equation 18b are from inertia ($\partial_t\mathbf{V}$ and $\mathbf{V}\cdot\nabla\mathbf{V}$), rotation ($2\mathbf{\Omega}\times\mathbf{V}$), pressure ($p_c$), buoyancy ($C\mathbf{g}_e$), magnetic field ($\mathbf{J}\times\mathbf{B}/\rho_0$), and viscosity ($\nu_T\nabla^2\mathbf{V}$). Thermal and compositional buoyancy, combined in the

codensity C (Braginsky and Roberts, 1995), maintains the flow and the magnetic field; see *Core Dynamo*.

The Coriolis force is generally more significant than the inertial and viscous forces. This is indicated by the smallness of the Ekman and Rossby numbers:

$$Ro = \mathcal{V}/\Omega\mathcal{L}. \tag{19}$$

See Equation 2c for the definition of E. From $\mathcal{V} = 10^{-4}$ m s^{-1}, $\mathcal{L} = r_o$ and $\nu_T = 10^{-2}\,\mathrm{m^2\,s^{-1}}$ follow $Ro \approx 10^{-6}$ and $E \approx 10^{-11}$. This suggests that the inertial and viscous terms can be safely omitted from Equation 18b, except on small length scales.

If the inertial and viscous forces are ejected from Equation 18b, it becomes

$$2\rho_0\mathbf{\Omega}\times\mathbf{V}^{\mathrm{N}} = -\boldsymbol{\nabla}p_c + \rho_0\mathcal{C}\mathbf{g}_{\mathrm{e}} + \mathbf{J}\times\mathbf{B}, \tag{20a}$$

where $^{\mathrm{N}}$ stands for "non-geostrophic," and "geostrophic" is defined below. Equations 18a and 20a define the "magnetostrophic approximation," often used to describe the quasi-steady macroscales of core MHD. As the viscous term has been ejected, the only boundary condition that $\mathbf{V}^{\mathrm{N}}$ must obey is

$$\mathbf{n}\cdot\mathbf{V}^{\mathrm{N}} = 0, \quad \text{on the CMB and ICB.} \tag{20b}$$

The full boundary conditions of continuous $\mathbf{B}$ and $\mathbf{n}\times\mathbf{E}$ still apply. Because $\partial_t\mathbf{V}$ has been ejected from Equation 20a, there are no Alfvén waves. Instead, the system evolves on the much longer ageostrophic time scale,

$$\tau^{\mathrm{N}} = 2\Omega\mathcal{L}^2/V_{\mathrm{A}}^2 = \tau_\eta/\Lambda, \qquad \text{where } \tau_\eta = \mathcal{L}^2/\eta \approx 10^5 \text{ years} \tag{20c,d}$$

is the free decay time for magnetic fields of scale $\mathcal{L}$, and Λ is the "Elsasser number":

$$\Lambda = V_{\mathrm{A}}^2/2\Omega\eta, \quad \text{where} \quad V_{\mathrm{A}} = \mathcal{B}/\sqrt{(\mu_0\rho_0)} \tag{20e,f}$$

is the Alfvén velocity. Elsasser (1946) suggested that $\mathcal{B}$ is determined by a balance of Lorentz and Coriolis forces. Taking $\mathcal{J} \approx \sigma\mathcal{V}\mathcal{B}$, this implies $\Lambda = 1$, $\mathcal{B} \approx 2$ mT, and $V_{\mathrm{A}} \approx 2\,\mathrm{cm\,s^{-1}}$. It also gives $\tau^{\mathrm{N}} \approx \tau_\eta \approx 2\times10^5$ years for $\mathcal{L} = r_o$.

In cylindrical coordinates (s, ϕ, z), the ϕ-component of Equation 20a is

$$2\Omega\rho_0 V_s^{\mathrm{N}} = -\partial_\phi p_c + (\mathbf{J}\times\mathbf{B})_\phi. \tag{21a}$$

Integrate this over the surface, $\mathcal{C}(s)$, of the circular cylinder of radius s ($> r_i$) coaxial with Oz. The left-hand-side vanishes by mass conservation, as can be verified by integrating Equation 18a over the interior, $\mathcal{I}(s)$, of $\mathcal{C}(s)$ and applying Equation 20b to $\mathcal{N}(s)$ and $\mathcal{S}(s)$, the spherical caps of $\mathcal{C}(s)$ on the CMB that complete the boundary of $\mathcal{I}(s)$. It follows that

$$\int_{\mathcal{C}(s)} (\mathbf{J}\times\mathbf{B})_\phi \,\mathrm{dA} = 0. \tag{21b}$$

If $s < r_i$, there are two cylinders, $\mathcal{C}^N(s)$ and $\mathcal{C}^S(s)$, of radius s to the north and south of the SIC for which

$$\int_{\mathcal{C}^N(s)} (\mathbf{J}\times\mathbf{B})_\phi \,\mathrm{dA} = 0, \quad \int_{\mathcal{C}^S(s)} (\mathbf{J}\times\mathbf{B})_\phi \,\mathrm{dA} = 0. \tag{21c,d}$$

Equations 20b–d are examples of "Taylor's constraint" (Taylor, 1963). The cylinders $\mathcal{C}(s)$ are termed "Taylor cylinders." Of these, $\mathcal{C}(r_i)$ is the tangent cylinder (TC).

It is obviously possible to assign a $\mathbf{J}$ which creates a $\mathbf{B}$ that contradicts Equations 21b–d, at least initially. This shows that Equation 20a is an oversimplification. That approximation rested on discarding the inertial force in comparison with the Coriolis force. Consider however the class of "geostrophic flows":

$$\mathbf{v} = \upsilon(s,\ t)\,\mathbf{1}_\phi. \tag{22a}$$

The corresponding Coriolis acceleration is

$$2\rho_0\mathbf{\Omega}\times\mathbf{v} = -\boldsymbol{\nabla}\mathcal{X}, \quad \text{where} \quad \mathcal{X} = 2\Omega\rho_0\int \upsilon(s,t)\,\mathrm{d}s \tag{22b,c}$$

can be absorbed into p_c. Coriolis forces are therefore totally ineffective when they act on geostrophic flows. Other forces previously abandoned in comparison with Coriolis forces become influential, especially the inertial forces, which must be restored when analyzing the geostrophic part of core flow. This recovers the Alfvén wave, or something very like it, called the "torsional wave." They share a common time scale:

$$\tau_{\mathrm{A}} = r_o/V_{\mathrm{A}} \approx 6 \text{ years}. \tag{22d}$$

That this is also the time scale $\mathrm{t_{LOD}}$ of the semi-decadal variations of in Figures 1a, b may not be a coincidence, as argued by Gillet et al. (2010).

The geostrophic part $\mathbf{v}$ of $\mathbf{V}$ can be extracted from $\mathbf{V}$ by taking the "geostrophic average," $\langle V_\phi\rangle$, of V_ϕ: for $s > r_i$, this average is defined by

$$\upsilon = \langle V_\phi\rangle \equiv \frac{1}{\widehat{A}(s)}\int_{\mathcal{C}(s)} V_\phi \,\mathrm{dA}, \quad \text{so that} \quad \mathbf{V}^{\mathrm{N}} = \mathbf{V} - \upsilon\mathbf{1}_\phi, \tag{22e}$$

where $\widehat{A}(s) = 4\pi s z_1$ is the area of $\mathcal{C}(s)$, and $z_1(s) = \sqrt{\left(r_o^2 - s^2\right)}$ is the semi-length of its sides. The axial angular momentum of the FOC is carried by υ. Therefore, insofar as the rotation of the SIC is locked to that of the fluid in the TC, the angular momentum, $M_z + \widetilde{M}_z$, of the entire core can be derived from the zonal part of the inferred core surface flow. The LOD record provides $\widehat{M}_z$. Therefore Equation 1h can be tested: $\widehat{M}_z = -(M_z + \widetilde{M}_z)$, Results have been gratifying; see Jault et al. (1988), Jackson (1997) and Figure 1c above. The previous section indicates however that the mantle and SIC are not locked together but take part in

a gravitational oscillation having a period (4–9 years) similar to the torsional wave period $\tau_A \approx 6$ years. The implied convolvement of gravitational and magnetic coupling complicates the task of extracting information about either; see Buffett et al. (2009).

In a torsional wave, the geostrophic cylinders are in relative angular motion about their common (polar) axis; see Figure 2a. The response **b** of **B** to the motion **v** can, as for an Alfvén wave, be visualized using the frozen flux theorem, the field lines behaving like elastic strings threading the cylinders together and opposing their relative motion; see Figure 2b. The resulting torque on a cylinder supplies the restoring force for a wave, the mass of the cylinders providing the inertia. Whenever **J** and **B** contradict Equations 21b–d, a torsional wave is launched that travels in the $\pm s$-indirections.

The canonical torsional wave equation is

$$\frac{\partial^2 \zeta}{\partial t^2} = \frac{1}{s^2 \widehat{A}(s)} \frac{\partial}{\partial s}\left[s^2 \widehat{A}(s) V_A^2(s) \frac{\partial \zeta}{\partial s}\right], \tag{23}$$

where $\zeta(s, t) = \upsilon/s$ is the angular velocity of $\mathcal{C}(s)$ and $V_A(s) = \mathcal{B}_s(s)/(\mu_0 \rho_0)^{1/2}$ is the Alfvén velocity based on the mean $\left(B_s^N\right)^2$ over $\mathcal{C}(s)$: $\mathcal{B}_s^2(s) = \left\langle \left(B_s^N\right)^2 \right\rangle$. Equation 23 is called canonical because it displays the essential nature of torsional waves clearly. It is however not only incomplete but also ignores magnetic coupling to the mantle and SIC. Equation 23 presupposes that the field, $\mathbf{B}^N$, on which the waves ride is axisymmetric. In this case, Equation 23 has a severe singularity at $s = 0$ which excludes physically acceptable solutions. This difficulty can be evaded by supposing that the TC rotates as a solid body, as suggested by Braginsky (1970), and by applying Equation 23 only in XTC. For general, nonaxisymmetric $\mathbf{B}^N$, the regular singularity at $s = 0$ is harmless, but unfortunately Equation 23 is then incomplete. The terms missing from Equation 23 represent the transmission of torque from one Taylor cylinder to another by the potential field outside the core. As the terms are troublesome if retained, they are usually abandoned, with an unsubstantiated claim that they are too small to be worth keeping. Whether they are retained or abandoned, the wave equation admits normal mode solutions, i.e., solutions in which ζ is proportional to $\exp(-\imath\omega t)$, where every ω is real, as shown in RA12. When magnetic coupling to the mantle is included, ω acquires a negative imaginary part, representing the ohmic losses in the mantle. The inclusion of magnetic coupling is highly relevant to our focus here, but it clearly adds another layer of complexity.

In view of these theoretical obstacles, the reader may wonder whether computer simulation would not provide a simpler approach. It is however difficult to extract evidence of torsional waves from geodynamo simulations. This is because it is not yet possible to attain geophysically realistic magnetic Prandtl numbers, Pm, in numerical integrations. The importance of viscous damping of torsional waves can be assessed by the ratio of the torsional wave time scale, $\tau_A = r_o/V_A$, to the spin-up time scale, $\tau_{SU} = \sqrt{\left(r_o^2/2\Omega\nu\right)}$, which is their viscous decay time; see Roberts and Soward (1972). This ratio,

$$\tau_A/\tau_{SU} = (2\Omega\nu)^{1/2}/V_A = \sqrt{(Pm/\Lambda)}, \tag{24}$$

is small for the Earth ($\sim 10^{-3}$) but inconveniently large in simulations ($\gtrsim 0.1$). See Wicht and Christensen (2010) for recent simulations of torsional waves.

Space limitations do not permit the mathematical theory of torsional waves to be presented here; see Braginsky (1970), Roberts and Soward (1972), Jault (2003), Dumberry (2007) and RA12. The principal aim in what follows is to outline the underlying physics, that has been employed in theoretical studies, and that will have to be incorporated in numerical models in the future, when computer technology has advanced far enough to permit core MHD to be modeled more faithfully. Our discussion here sidesteps interesting and as yet incompletely answered questions, the first of which is whether torsional waves are involved in any essential way with the semi-

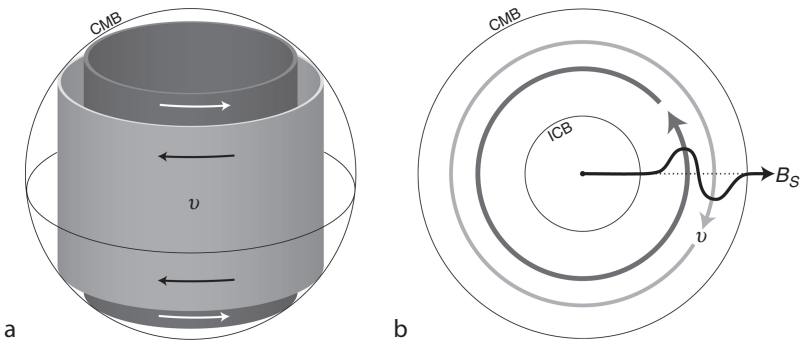

Core-Mantle Coupling, Figure 2 Schematics showing (**a**) geostrophic flows in the core, V^g, and (**b**) plan view of an initially cylindrical magnetic field (*dashed line*) distorted by *v*. The restoring Lorentz torques on the distorted magnetic field, B_s (*solid line*), lead to the cylindrical propagation of torsional waves (Adapted from Dumberry, 2007).

decadal LOD periodicity; might not the gravitational oscillation described in the last section be mainly responsible? The answer is unclear but core field strengths of 2 mT suggest that torsional waves very effectively link together geostrophic motions throughout the core, and that torsional waves therefore necessarily accompany gravitational oscillations. This obviously does not imply that torsional waves couple well to the mantle; if the mantle were an electrical insulator, there would be no magnetic coupling of core and mantle at all. The waves would then be detectable only through the inferred core surface motion. Strong magnetic coupling of the waves to the mantle raises difficult questions about both the excitation and dissipation of the waves. As shown below, the waves are mainly and heavily damped by ohmic dissipation in the mantle. What maintains the waves against this energy loss? No definitive answer has been given to this very significant question. Core turbulence may be directly responsible, or indirectly through the Reynolds magneto-stresses it exerts on the SIC or on the TC. Buffett et al. (2009) find evidence for wave generation at the TC. Core turbulence would presumably excite many damped normal modes. This might help to explain some of the recently discovered short time scales of core surface motions (Olsen and Mandea, 2008; Finlay et al., 2010). It has not been established unequivocally that the 6 year period is the fundamental mode. Though often questioned, evidence of a 60 periodicity exists, This longer period signal might be representative of the fundamental mode but would require current estimates of $\mathcal{B}_s(s)$ to be revised downward.

These matters are beyond the scope of this review. We shall merely sketch, mostly in a qualitative way, the approximate theory that is currently the most complete. We also aim to expose its strengths and weaknesses.

Underlying the entire theory is the idea that core flow can be neatly separated into geostrophic motions of short time scale, τ_A, and non-geostrophic motions of long time scale τ^{N}obeying Equation 20a. In other words, the theory focusses on the large length scales of core flow, in the belief that this includes the fundamental torsional wave mode of greatest interest. The torsional wave therefore rides on a flow satisfying Taylor's constraints Equations 21a–c. Because the Lehnert number, $\lambda = \tau_A/\tau^{\mathrm{N}} = V_A/2\Omega r_o = \omega_A/2\Omega \approx 3 \times 10^{-5}$, is small, the time dependence of $\mathbf{B}^{\mathrm{N}}$ can be ignored in torsional wave theory.

It was pointed out earlier that torsional waves are geostrophic motions in which the inertial force is crucial. The first step in deriving the torsional wave equation is therefore to restore the time-dependent inertial force to Equation 21a, obtaining

$$\rho_0 s\partial_t V_\phi + 2\Omega\rho_0 s V_s = -\partial_\phi p_c + s(\mathbf{J}\times\mathbf{B})_\phi, \qquad (25a)$$

from which $\partial_t\zeta$ is extracted, by taking the geostrophic average; see Equation 22e.

The evaluation of $\langle \mathbf{J}\times\mathbf{B}\rangle_\phi$ is simplified because E is small and the Lundquist number, $Lu = \tau_\eta/\tau_{\mathrm{A}} = V_{\mathrm{A}} r_o/\eta \approx 3\times 10^4$, of the waves is large. In a first approximation, $E = Lu^{-1} = 0$. Then viscous and ohmic diffusion and the associated boundary conditions are discarded. In particular, the electric field created in the FOC by the waves simplifies to

$$\mathbf{e} = -\mathbf{v}\times\mathbf{B}^{\mathrm{N}} - \mathbf{V}^{\mathrm{N}}\times\mathbf{b} - \mathbf{v}\times\mathbf{b}, \qquad (25b)$$

where $\mathbf{b}$ is the magnetic field of the waves. The term $-\mathbf{V}^{\mathrm{N}}\times\mathbf{B}^{\mathrm{N}}$ does not appear because it already acts on the Taylor state. The last term in Equation 25b is also ignored because the wave amplitude is assumed to be small. The ratio of $-\mathbf{V}^{\mathrm{N}}\times\mathbf{b}$ to $-\mathbf{v}\times\mathbf{B}^{\mathrm{N}}$ is of order $A^{\mathrm{N}}[b/\upsilon\sqrt{(\mu_0\rho_0)}]^{-1}$, where $A = V/V_{\mathrm{A}}$ is the Alfvén number, which for the non-geostrophic flow is about 0.1 (see above). As in an Alfvén wave, $\upsilon = \mathrm{O}[b/\sqrt{(\mu_0\rho_0)}]$, so that $|\mathbf{V}^{\mathrm{N}}\times\mathbf{b}| \approx 0.1|\mathbf{v}\times\mathbf{B}^{\mathrm{N}}|$. This, combined with the fact that the inclusion of $-\mathbf{V}^{\mathrm{N}}\times\mathbf{b}$ in $\mathbf{e}$ adds severe complications, encourages the neglect of $-\mathbf{V}^{\mathrm{N}}\times\mathbf{b}$ in Equation 25b, leaving

$$\mathbf{e} = -\mathbf{v}\times\mathbf{B}^{\mathrm{N}}. \qquad (25c)$$

The mantle and core are linked across a boundary layer of Ekman-Hartmann type; e.g., see Dormy et al. (2007). Because $Pm \ll 1$, this has a double structure. Viscosity acts only in an Ekman layer of thickness $d_\nu = \sqrt{(\nu/2\Omega)} \approx 0.1$ m; magnetic diffusion acts in a layer whose thickness is comparable with the EM skin depth, $d_\eta = \left(\frac{1}{2}|\omega|\mu_0\sigma\right)^{-1/2} \approx 10\,\mathrm{km}$. We therefore call this a "magnetic diffusion layer" (MDL), even though Coriolis and Lorentz forces affect its structure too. In the MDL, Equation 25c is replaced by

$$\mathbf{e} = -\mathbf{v}\times\mathbf{B}^{\mathrm{N}} - \eta\boldsymbol{\nabla}\times\mathbf{b} \approx -\mathbf{v}\times\mathbf{B}^{\mathrm{N}} - \eta\mathbf{1}_r\times\partial_r\mathbf{b}. \qquad (26)$$

As $d_\eta/d_\nu \gg 1$, the Ekman layer is only a tiny part of the MDL. Ekman-Hartmann theory simplifies by discarding the Ekman part, setting $\nu = 0$ and abandoning the no-slip boundary conditions. The structure of the MDL still depends on rotation, and on the Elsasser number, Λ, defined in Equation 20e.

The boundary layers play a vital role in linking ζ in the main bulk of the FOC to $\widehat{\mathbf{b}}$ on the CMB and $\underline{\mathbf{b}}$ on the ICB. They are therefore essential in determining $\widehat{\boldsymbol{\Gamma}}^M$ and $\underline{\boldsymbol{\Gamma}}^M$. At the CMB, $\mathcal{B} \approx 0.5$ mT and $\Lambda \approx 0.07$. The prevailing magnetic field, $\mathbf{B}^{\mathrm{N}}$, therefore has very little effect on the boundary layer, which is controlled almost entirely by Coriolis forces and magnetic diffusion. At the ICB, where $\mathcal{B}$ may be even an order of magnitude greater than at the CMB, $\Lambda > 1$, and Lorentz forces are too significant to ignore in the boundary layer. Further details are given in RA12.

The torque exerted by the waves on the mantle is proportional to the electrical conductivity, $\widehat{\sigma}(\nu, \theta, \phi)$, of the mantle, which we assume is nonzero only in the layer

$r_o < r < r_1 = r_o + d$ at the base of the mantle. The conductance of this layer is

$$\widehat{\Sigma}(\theta,\phi) = \int_{r_o}^{r_1} \widehat{\sigma}\ (r,\theta,\phi)\, dr. \tag{27a}$$

It is commonly assumed that $10^7 S < \widehat{\Sigma} < 10^9$S; we take $\widehat{\Sigma} = 10^8$S below.

Electric currents, $\widehat{\mathbf{j}}$, flow in the mantle, $\widehat{\mathrm{V}}$, either by leaking from the core or by electromagnetic induction, through the time dependence of the EM field on the CMB. We shall be interested in the penetration of the fields **b** and **e** of the waves, at frequencies ω of order 5×10^{-8} s^{-1}. The resulting magnetic and electric fields, $\widehat{\mathbf{b}}$ and $\widehat{\mathbf{e}}$, in the mantle depend on ω and on L, the horizontal length scale imposed by **b** and **e** on the CMB. Associated with ω is the skin depth of the mantle:

$$\widehat{d}_\eta = \left(\frac{1}{2}|\omega|\mu_0\widehat{\sigma}_o\right)^{-1/2}. \tag{27b}$$

Starting with Glatzmaier and Roberts (1995), theoreticians have usually simplified EM theory in the mantle by adopting the "thin-layer approximation" (TLA). This originated from the modeling of laboratory MHD experiments (see, e.g., Müller and Bühler, 2001). It is easily applied and therefore popular, although the conditions for its validity are seldom mentioned or questioned. The TLA demands that $d \ll \widehat{d}_\eta\ (\ll L)$. The horizontal part, $\widehat{\mathbf{e}}_\mathrm{H}$, of the electric field $\widehat{\mathbf{e}}$ is then independent of r, so that

$$\widehat{\mathbf{j}}_\mathrm{H} = \widehat{\sigma}\,\widehat{\mathbf{e}}_\mathrm{H}, \quad \text{and} \quad \widehat{\mathcal{J}} = \widehat{\Sigma}\,\widehat{\mathbf{e}}_\mathrm{H}, \tag{27c,d}$$

where $\widehat{\mathcal{J}}$ is the total horizontal current carried by the layer.

It may be helpful to visualize the TLA as a mathematical limit, $d \to 0$, $\widehat{\sigma} \to \infty$ with $\widehat{\Sigma}$ held fixed. Then $\widehat{\mathcal{J}}$ is a surface current responsible for a discontinuity in the magnetic field. If $\check{\mathbf{b}}(= -\boldsymbol{\nabla}\check{\mathrm{w}})$ is the potential field above the conducting layer,

$$\begin{aligned}\check{\mathbf{b}}(r_o,\theta,\phi) - \widehat{\mathbf{b}}(r_o,\theta,\phi) &= \mu_0\widehat{\mathcal{J}}(\theta,\phi)\times\mathbf{1}_r \\ &= \mu_0\widehat{\Sigma}(\theta,\phi)\widehat{\mathbf{e}}_\mathrm{H}(r_o,\theta,\phi)\times\mathbf{1}_r.\end{aligned} \tag{27e}$$

The potential field does not affect the torque, $\mathbf{\Gamma}^M$, on the mantle, although it does contribute to the torque that each Taylor cylinder exerts on the others.

We contrast two proposed conductivity distributions. Buffett et al. (2002) inferred from their studies of nutational resonances that d is only 200 m and that $\widehat{\sigma} = 3 \times 10^5$ S m^{-1}, which is comparable to the core conductivity σ, and gives $\widehat{d}_\eta = 10$ km. The TLA should therefore be excellent in most applications. In contrast, the laboratory experiments of Ohta et al. (2008) suggest $\widehat{\sigma} = 100$ S m^{-1} and $d = 3 \times 10^5$ m; see also Yoshino (2010). This gives $\widehat{d}_\eta = 2 \times 10^6$ m, so it is doubtful if the TLA can be validly applied. The similar conductances of the models ($\widehat{\Sigma} = 3/6 \times 10^7$ S) are insufficient to justify the use of the TLA.

This completes our critique of the basics of torsional wave coupling to the mantle. Some of its consequences are unexpected; but most are not. Even dimensional reasoning leads to

$$\begin{aligned}&\widehat{\Gamma}_z^M = \widehat{\Gamma}_0^M(\overline{\zeta} - \widehat{\zeta}), \\ &\text{where } \widehat{\Gamma}_0^M = O\left(r_o^4\widehat{\Sigma}\mathcal{B}_o^2\right) \approx 4\times10^{27}\,\text{Nms},\end{aligned} \tag{28a,b}$$

for $\mathcal{B} = 0.5$mT . Here $\mathcal{B}_o^2$ is an average of $\left(B_r^N\right)^2$ over the CMB, and $\overline{\zeta}$ is defined by:

$$\overline{\zeta}(t) = \frac{1}{s^2\widehat{A}(s)}\int_0^{r_o} s^2\widehat{A}(s)\zeta(s,t)\mathrm{d}s \tag{28c}$$

Perhaps unexpectedly, the boundary layer on the CMB described above reduces $\widehat{\Gamma}_0^M$ by a factor of $\Sigma/(\Sigma + \widehat{\Sigma})$, where Σ is the conductance of the boundary layer, defined by

$$\Sigma = \frac{1}{2}(1+\imath\varsigma)\sigma d_\eta = (1+\imath\varsigma)(\sigma/2\mu_0|\omega|)^{1/2}, \tag{28d}$$

and $\varsigma = \mathrm{sgn}(\omega)$. This gives $|\Sigma| \approx 3 \times 10^9$ S, which is comparable with $\widehat{\Sigma}$. Ignoring this factor, the magnetic interaction of mantle and FOC is governed by

$$\widehat{C}d_t\widehat{\zeta} = \widehat{\Gamma}_0^M(\overline{\zeta} - \widehat{\zeta}), \qquad Cd_t\overline{\zeta} = -\widehat{\Gamma}_0^M\left(\overline{\zeta} - \widehat{\zeta}\right), \tag{28e,f}$$

where $C = 9.08 \times 10^{36}$ kg m^2 is the polar moment of inertia of the solidly rotating FOC. These equations provide an estimate of the e-folding time, $\widehat{\tau}_\eta$, taken by mantle conduction to kill ζ and $\widehat{\zeta}$: $\widehat{\tau}_\eta = C\widehat{C}/(C+\widehat{C})\widehat{\Gamma}_0^M \approx 64$ years. This is greater than the time taken by the waves to cross the core, which is $\tau_\mathrm{A} = r_o/V_\mathrm{A} \approx 5.6$ years, for $\mathcal{B} = 2$mT.

If we take $\delta\widehat{\zeta} \approx 3 \times 10^{-12}$s^{-1}, as indicated by the LOD data of the first section above, Equations 28e, f suggest that $\overline{\zeta} - \widehat{\zeta} \approx (\widehat{C}+C)\widehat{\zeta}/C$ is about 2×10^{-11} s^{-1}, so that $r_o(\overline{\zeta} - \widehat{\zeta}) \approx 7 \times 10^{-5}$ m s^{-1}, which is less than, but comparable with, the inferred core surface flow. It also gives $\widehat{\Gamma}_z^M \approx 8 \times 10^{16}$ Nm. This increases to the target torque if we take $\widehat{\Sigma} = 1.2 \times 10^9$ S, but that reduces $\widehat{\tau}_\eta$ to 5.3 years, which is less than τ_A.

This highlights a difficulty that might be called the "magnetic coupling paradox," and quantified by a quality factor:

$$\Pi = \widehat{\tau}_\eta/\tau_\mathrm{A} = (\mathcal{B}/\mathcal{B}_o)^2\left(\mu_0\widehat{\Sigma}V_\mathrm{A}\right)^{-1}. \tag{29}$$

There is a window for $\widehat{\Sigma}$, that may be narrow or nonexistent, in which $\widehat{\Gamma}_z^M$ is large enough to explain variations in LOD by torsional waves, but simultaneously is small enough to ensure that $\Pi > 1$ so that the waves are not over

damped by mantle conduction. According to the admittedly imprecise, order of magnitude estimates made here, the window is nonexistent. For the target torque to be reached or exceeded, $\widehat{\Gamma} \gtrsim 1.2 \times 10^9$ S, but $\Pi > 1$ requires $\widehat{\Gamma} \lesssim 1.1 \times 10^9$ S. See also Dumberry and Mound (2008).

So far the existence of the SIC has been ignored, almost totally. We have however recognized that, for $s < r_i$, two Taylor cylinders exist, $\mathcal{C}^N(s)$ and $\mathcal{C}^S(s)$, in which $\zeta^N(s)$ and $\zeta^S(s)$ may be expected to differ. For simplicity, we assume here that they are equal. To evaluate $\widetilde{\Gamma}_z$, it is necessary to link $\mathbf{b}$ to $\widetilde{\mathbf{b}}$ across a boundary layer strongly influenced by Λ. An analysis of the boundary layer leads to (see RA12)

$$\widetilde{b}_\phi = \mu_0 \widetilde{\sigma} \widetilde{d}_\eta s B_r^N (\overline{\zeta} - \widetilde{\zeta}) \quad \text{on} \quad r = r_i, \tag{30a}$$

where $\widetilde{\zeta}$ is the angular velocity of the SIC, and $\widetilde{d}_\eta = \left(\frac{1}{2}|\omega|\mu_0\widetilde{\sigma}_i\right)^{-1/2} \approx d_\eta \approx 10$ km. This leads to an expression for $\widetilde{\Gamma}_z^M$, in which the main part that couples to the TC is

$$\widetilde{\Gamma}_z^M = \widetilde{\Gamma}_0^M (\overline{\zeta} - \widehat{\zeta}), \quad \text{where} \quad \widetilde{\Gamma}_0^M = \mathrm{O}\left(r_i^4 \widetilde{\sigma} \widetilde{d}_\eta \mathcal{B}_i^2\right); \tag{30b,c}$$

cf. Equations 28a, b. For $\mathcal{B}_i = 5$ mT, $\widetilde{\Gamma}_0^M \approx 2 \times 10^{29}$ Nms. This large torque acts on the SIC whose moment of inertia is less than $10^{-3}\widehat{C}$. The coupling time, $\widetilde{\tau}_\eta$, is therefore very much less than $\widehat{\tau}_\eta$. Equations analogous to Equation 28a, b give (for $\widetilde{\sigma} = \sigma$)

$$\widetilde{\tau}_\eta \approx \widetilde{C}/|\widetilde{\Gamma}_0^M| \approx 4 \text{ days}. \tag{30d}$$

This is the time taken for a mismatch between ζ and $\widetilde{\zeta}$ to be wiped out by magnetic torques. Clearly the coupling between TC and SIC is substantial at frequencies of order ω_A. This supports the opinion, advanced several times in this review, that on semi-decadal time scales, the TC is effectively locked to the SIC in its rotation about Oz.

Synthesis

In this review we have analyzed the various ways in which Earth's core is coupled to the mantle and have presented estimates of the amplitudes of these couplings in order to show which may plausibly explain the available LOD data. In our first section, we provide observational evidence for core-mantle coupling. We show that Earth's rotation rate has a roughly semi-decadal time variability, such that the LOD fluctuates at the ms level. To explain these LOD fluctuations, an internal coupling must exist between the mantle and the core that provides torques of order 10^{18} Nm, which we named "the target torque."

In the later text, we develop estimates of the strength of the viscous, topographic, gravitational, and electromagnetic torques. Only the viscous torque, Γ_z^V, appears to be too weak to explain the LOD signal. This is true even when we allow for the enhanced coupling that turbulence can provide.

The topographic torque on the mantle, $\widehat{\Gamma}_z^T$, is created by core flow interacting with bumps on the CMB. In analyzing $\widehat{\Gamma}_z^T$, it became clear that exchange of angular momentum with the SIC is significant. Order of magnitude arguments showed that potentially the largest part of $\widehat{\Gamma}_z^T$ is $\widehat{\Gamma}_{a,z}^T$, which is produced by the gravitational field of density anomalies in the mantle and possibly SIC, including bumps on their surfaces. This part of $\widehat{\Gamma}_z^T$ is therefore intimately related to the gravitational torque $\widehat{\Gamma}_z^G$. When the two are treated together as $\widehat{\Gamma}_{a,z}^{G+T}$, there is an equal but opposite torque, $\widetilde{\Gamma}_{a,z}^{G+T}$ on the SIC. Gravitational oscillations (Buffett, 1996) occur when the system is perturbed from a state of minimum gravitational energy in which $\widehat{\Gamma}_{a,z}^{G+T} = \widetilde{\Gamma}_{a,z}^{G+T} = 0$. An oscillation period of $\tau^\mathrm{G} = 4.1$ years was derived. If, as seems likely, strong magnetic coupling exists between the tangent cylinder (TC) and the SIC, the gravitational oscillation period increases to $\tau_\mathrm{TC}^G = 8.9$ years.

The remaining part of $\widehat{\Gamma}_z^T$ is $\widehat{\Gamma}_{c,z}^T$, and is produced by core convection. Its importance is uncertain. From what is known today, $\Gamma_{c,z}^T$ may be 0 Nm or may exceed the target torque (cf. Kuang and Bloxham, 1997; Hide, 1998; Jault and Le Mouël, 1999; Kuang and Chao, 2001).

A simple model of torsional waves traversing FOC can explain oscillations of period, $\tau \approx 6$ years, but there is a paradox: The target torque cannot be attained by magnetic coupling between the waves and the mantle unless a dimensionless "paradox parameter," Π, defined in Equation 29, is large enough. If this parameter is too large, however, the waves are damped out before they can cross the core. Whether the core can evade the paradox seems uncertain.

The topographic, gravitational and magnetic torques all have significant uncertainties in their amplitudes, but the target torque falls within these uncertainties, i.e., conceivable any of them could explain the semi-decadal LOD signals. The coupling processes may be convolved. The recent model of Buffett et al. (2009) allows for this, but argues that the gravitational torque dominates. In contrast, Gillet et al. (2010) infer that torsional oscillations in the FOC can explain the LOD observations without strong gravitational coupling. Improvements in data and modeling of Earth's rotation (e.g., Gross, 2009), the geomagnetic field (e.g., Hulot et al., 2002; Jackson, 2003), core seismology (e.g., Dai and Song, 2008), and the time-variations in the gravity field (e.g., Velicogna and Wahr, 2006; Dumberry, 2010) will all prove important in testing these core-mantle coupling arguments.

This review has focussed on explaining variations in LOD owing to internal coupling between the mantle and core. This coupling produces changes primarily in the axial angular rotation rate, Ω_z, on semi-decadal time scales. Detailed measurements now exist of variations in Earth's full rotation vector on many time scales (e.g., Gross, 2007), with the different directional components

providing information on different geophysical phenomena (e.g., Mathews et al., 2002). Furthermore, rotation vector and magnetic field measurements now exist for other planets (e.g., Margot et al., 2007; Uno et al., 2009), and will improve in quality in the coming decades. Such measurements will allow the development of models of deep interior structure and dynamics in planetary bodies throughout the solar system (e.g., Tyler, 2008; Noir et al., 2009; Goldreich and Mitchell, 2010).

Acknowledgments

We thank Richard Gross, Richard Holme, and Andrew Jackson for sharing their insights and their data. We are also grateful to Bruce Buffett and the referee (Mathieu Dumberry) for giving helpful advice.

Bibliography

Abarca del Rio, R., Gambis, R., and Salstein, D. A., 2000. Interannual signals in length of day and atmospheric angular momentum, *Annales Geophysicae*, **18**, 347–364.

Alboussière, T., Deguen, R., and Melzani, M., 2010. Melting induced stratification above the Earth's inner core due to convective translation. *Nature*, **466**, 744–747.

Anufriev, A. P., and Braginsky, S. I., 1975. Influence of irregularities of the boundary of the Earth's core on the velocity of the liquid and on the magnetic field. *Geomagnetism and Aeronomy*, **15**, 754–757.

Anufriev, A. P., and Braginsky, S. I., 1977a. Influence of irregularities of the boundary of the Earth's core on the fluid velocity and the magnetic field, II. *Geomagnetism and Aeronomy*, **17**, 78–82.

Anufriev, A. P., and Braginsky, S. I., 1977b. Influence of irregularities of the boundary of the Earth's core on the fluid velocity and the magnetic field, III. *Geomagnetism and Aeronomy*, **17**, 742–750.

Braginsky, S. I., 1970. Torsional magnetohydrodynamic vibrations in the Earth's core and variations in day length. *Geomagnetism and Aeronomy*, **10**, 1–8.

Braginsky, S. I., 1984. Short-period geomagnetic secular variation. *Geophysical and Astrophysical Fluid Dynamics*, **30**, 1–78.

Braginsky, S. I., 1999. Dynamics of the stably stratified ocean at the top of the core. *Physics of the Earth and Planetary Interiors*, **111**, 21–34.

Braginsky, S. I., and Roberts, P. H., 1995. Equations governing convection in Earth's core and the Geodynamo. *Geophysical and Astrophysical Fluid Dynamics*, **79**, 1–97.

Braginsky, S. I., and Roberts, P. H., 2007. Anelastic and Boussinesq approximations. In Gubbins, D., and Herrero-Bervera, E. (eds.), *Encyclopedia of Geomagnetism and Paleomagnetism*. Heidelberg: Springer, pp. 11–19.

Brito, D., Aurnou, J. M., and Cardin, P., 2004. Turbulent viscosity measurements relevant to planetary core-mantle dynamics. *Physics of the Earth and Planetary Interiors*, **141**, 3–8.

Buffett, B. A., 1996. Gravitational oscillations in the length of day. *Geophysical Research Letters*, **23**, 2279–2282.

Buffett, B. A., 1997. Geodynamic estimates of the viscosity of the Earth's inner core. *Nature*, **388**, 571–573.

Buffett, B. A., 1998. Free oscillations in the length of day: inferences on physical properties near the core-mantle boundary. *Geodynamics*, **28**, 153–165.

Buffett, B. A., 2010. Chemical stratification at the top of Earth's core: constraints from nutation observations. *Earth and Planetary Science Letters*, **296**, 367–372.

Buffett, B. A., and Christensen, U. R., 2007. Magnetic and viscous coupling at the core-mantle boundary; inferences from observations of the Earth's nutations. *Geophysical Journal International*, **171**, 145–152.

Buffett, B. A., and Glatzmaier, G. A., 2000. Gravitational braking of inner-core rotation in geo-dynamo simulations. *Geophysical Research Letters*, **27**, 3125–3128.

Buffett, B. A., Mathews, P. M., and Herring, T. A., 2002. Modeling of nutation and precession: effects of electromagnetic coupling. *Journal of Geophysical Research*, **107**, 2070, doi:10.1029/2000JB000056.

Buffett, B. A., Mound, J., and Jackson, A., 2009. Inversion of torsional oscillations for the structure and dynamics of Earth's core. *Geophysical Journal International*, **177**, 878–890.

Dai, W., and Song, X., 2008. Detection of motion and heterogeneity in Earth's liquid outer core. *Geophysical Research Letters*, **35**, L16311.

Davidson, P. A., 2001. *An Introduction to Magnetohydrodynamics*. Cambridge, UK: Cambridge University Press.

Davidson, P. A., 2004. *Turbulence*. Oxford, UK: Oxford University Press.

de Wijs, G. A., Kresse, G., Vočadlo, I., Dobson, D. P., Alfèe, D., Gillan, M. J., and Price, G. D., 1998. The viscosity of liquid iron at the physical conditions of Earth.s core. *Nature*, **392**, 805–807.

Defraigne, P., Dehant, V., and Wahr, J., 1996. Internal loading of an inhomogeneous compressible mantle with phase boundaries. *Geophysical Journal International*, **125**, 173–192.

Deleplace, B., and Cardin, P., 2006. Viscomagnetic torque at the core-mantle boundary. *Geophysical Journal International*, **167**, 557–566.

Dobson, D. P., Crichton, W. A., Vočadlo, I., Jones, A. P., Wang, Y., Uchida, T., Rivers, M., Sutton, S., and Brodhardt, J. P., 2000. In situ measurements of viscosity of liquids in the Fe-FeS system at high pressures and temperatures. *American Mineralogist*, **85**, 1838–1842.

Dormy, E., Roberts, P. H., and Soward, A. M., 2007. Core, boundary layers. In Gubbins, D., and Herrero Bervera, E. (eds.), *Encylopedia of Geomagnetism and Paleomagnetism*. Heidelberg: Springer, pp. 111–116.

Dumberry, M., 2007. Taylor's constraint and torsional oscillations. In Cardin, P., and Cugliandolo, L. F. (eds.), *Dynamos*. Amsterdam: Elsevier, pp. 383–401.

Dumberry, M., 2010. Gravity variations induced by core flows. *Geophysical Journal International*, **180**, 635–650.

Dumberry, M., and Mound, J., 2008. Constraints on core-mantle electromagnetic coupling from torsional oscillation normal modes. *Journal of Geophysical Research*, **113**, B03102, doi:10.1029/2007JB005135.

Elsasser, W. M., 1946. Induction effects in terrestrial magnetism, II. The secular variation. *Physical Review*, **70**, 202–212.

Fearn, D. R., Loper, D. E., and Roberts, P. H., 1981. Structure of the Earth's inner core. *Nature*, **292**, 232–233.

Finlay, C. C., Dumberry, M., Chulliat, A., and Pais, M. A., 2010. Short timescale core dynamics: theory and observations. *Space Science Reviews*, **155**, 177–218, doi:10.1007/s11214-010-9691-6.

Forte, A. M., Woodward, R. J., and Dziewonski, A. M., 1994. Joint inversion of seismic and geo-dynamic data for models of three-dimensional mantle heterogeneity. *Journal of Geophysical Research*, **99**, 21857–21877.

Gargett, A. E., 1984. Vertical eddy diffusivity in the ocean interior. *Journal of Marine Research*, **42**, 359–393.

Gillet, N., Jault, D., Canet, E., and Fournier, A., 2010. Fast torsional waves and strong magnetic field within the Earth's core. *Nature*, **465**(7294), 74–77, doi:10.1038/nature09010.

Glatzmaier, G. A., and Roberts, P. H., 1995. A three-dimensional convective dynamo solution with rotating and finitely

conducting inner core and mantle. *Physics of the Earth and Planetary Interiors*, **91**, 63–75.
Goldreich, P. M., and Mitchell, J. L., 2010. Elastic ice shells and synchronous moons: implications for cracks on Europa and non-synchronous rotation on Titan. *Icarus*, doi:10.1016-/j.icarus.2010.04.013.
Gross, R. S., 2001. A combined length-of-day series spanning 1832–1997: LUNAR97. *Physics of the Earth and Planetary Interiors*, **123**, 65–76.
Gross, R. S., 2007. Earth rotation variations – long period. In Herring, T. A. (ed.), *Physical Geodesy.* Oxford: Elsevier. Treatise on Geophysics, Vol. 3, pp. 239–294.
Gross, R. S., 2009. Ocean tidal effects on Earth rotation. *Journal of Geodynamics*, **48**, 219–225.
Heimpel, M. H., and Aurnou, J. M., 2007. Turbulent convection in rapidly rotating spherical shells: a model for equatorial and high latitude jets on Jupiter and Saturn. *Icarus*, **187**, 540–557.
Hide, R., 1969. Interaction between the earth's liquid core and solid mantle. *Nature*, **222**, 1055–1956.
Hide, R., 1998. A note on topographic core-mantle coupling. *Physics of the Earth and Planetary Interiors*, **109**, 91–92.
Hide, R., and James, I. N., 1983. Differential rotation produced by potential vorticity mixing in a rapidly rotating fluid. *Geophysical Journal of the Royal Astronomical Society*, **74**, 301–312.
Hide, R., Clayton, R. W., Hager, B. H., Speith, M. A., and Voorhies, C. V., 1993. Topographic core-mantle coupling and fluctuations in Earth's rotation. In Aki, K., and Dmowska, R. (eds.), *Relating Geophysical Structures and Processes: The Jeffreys Volume*. Washington, DC: AGU. Geophysical Monograph Series, Vol. 76, pp. 107–120.
Holme, R., 1998. Electromagnetic core-mantle coupling-I. Explaining decadal changes in the length of day. *Geophysical Journal International*, **132**, 167–180.
Holme, R., and de Viron, O., 2005. Geomagnetic jerks and a high-resolution length-of-day profile for core studies. *Geophysical Journal International*, **160**, 435–439.
Hulot, G., Eymin, C., Langlais, B., Mandea, M., and Olsen, N., 2002. Small-scale structure of the geodynamo inferred from Oersed and Magsat satellite data. *Nature*, **416**, 620–623.
Jackson, A., 1997. Time-dependency of tangentially geostrophic core surface motions. *Physics of the Earth and Planetary Interiors*, **103**, 293–311.
Jackson, A., 2003. Intense equatorial flux spots on the surface of Earth's core. *Nature*, **424**, 760–763.
Jacobs, J. A., 1953. The Earth's inner core. *Nature*, **172**, 297–298.
Jault, D., 2003. Electromagnetic and topographic coupling, and LOD variations. In Jones, C. A., Soward, A. M., and Zhang, K. (eds.), *Earth's Core and Lower Mantle*. London: Taylor and Francis, pp. 46–76.
Jault, D., and Le Mouël, J. L., 1989. The topographic torque associated with a tangentially geostrophic motion at the core surface and inferences on the flow inside the core. *Geophysical and Astrophysical Fluid Dynamics*, **48**, 273–296.
Jault, D., and Le Mouël, J. L., 1999. Comment on 'On the dynamics of topographic core-mantle coupling' by Weijia Kuang and Jeremy Bloxham. *Physics of the Earth and Planetary Interiors*, **114**, 211–215.
Jault, D., Gire, C., and LeMouel, J.-L., 1988. Westward drift, core motions and exchanges of angular momentum between core and mantle. *Nature*, **333**, 353–356.
Kawai, K., and Tsuchiya, T., 2009. Temperature profile in the lowermost mantle from seismological and mineral physics joint modeling. *Proceedings of the National Academy of Sciences of the United States of America*, doi:10.1073/pnas.0905920106.
Kuang, W.-J., and Bloxham, J., 1993. The effect of boundary topography on motions in the Earth's core. *Geophysical and Astrophysical Fluid Dynamics*, **72**, 161–195.
Kuang, W.-J., and Bloxham, J., 1997. On the dynamics of topographic core-mantle coupling. *Physics of the Earth and Planetary Interiors*, **99**, 289–294.
Kuang, W.-J., and Chao, B. F., 2001. Topographic core-mantle coupling in geodynamo modeling. *Geophysical Research Letters*, **28**, 1871–1874.
Loper, D. E., 2007. Turbulence and small-scale dynamics in the core. In Olson, P. L. (ed.), *Core Dynamics*. Amsterdam: Elsevier. Treatise on Geophysics, Vol. 8, pp. 187–206.
Love, J. J., and Bloxham, J., 1994. Electromagnetic coupling and the toroidal magnetic field at the core-mantle boundary. *Geophysical Journal International*, **117**, 235–256.
Margot, J. L., Peale, S. J., Jurgens, R. F., Slade, M. A., and Holin, I. V., 2007. Large longitude libration of Mercury reveals a molten core. *Science*, **316**, 710–714.
Mathews, P. M., Herring, T. A., and Buffett, B. A., 2002. Modeling of nutation and precession: new nutation series for nonrigid Earth and insights into the Earth's interior. *Journal of Geophysical Research*, **107**, 2068, doi:10.1029/2001JB000390.
Monnereau, M., Calvet, M., Margerin, L., and Souriau, A., 2010. Lopsided growth of Earth's inner core. *Science*, **328**, 1014–1017.
Morse, S. A., 1986. Adcumulus growth of the inner core. *Geophysical Research Letters*, **13**, 1466–1469.
Mound, J. E., and Buffett, B. A., 2003. Interannual oscillations in length of day: implications for the structure of the mantle and core. *Journal of Geophysical Research*, **108**, 2334, doi:10.1029/2002JB002054.
Mound, J. E., and Buffett, B. A., 2005. Mechanisms of core-mantle angular momentum exchange and the observed spectral properties of torsional oscillations. *Journal of Geophysical Research*, **110**, B08103, doi:10.1029/2004JB003555.
Mound, J., and Buffett, B., 2006. Detection of a gravitational oscillation in length-of-day. *Earth and Planetary Science Letters*, **243**, 383–389.
Müller, U., and Bühler, L., 2001. *Magnetofluiddynamics in Channels and Containers*. Heidelberg: Springer.
Noir, J., Hemmerlin, F., Wicht, J., Baca, S. M., and Aurnou, J. M., 2009. An experimental and numerical study of librationally driven flow in planetary cores and subsurface oceans. *Physics of the Earth and Planetary Interiors*, **173**, 141–152.
Ohta, K., Onada, S., Hirose, K., Sinmyo, R., Shimizu, K., Saya, N., Ohishi, Y., and Yasuhara, A., 2008. The electrical conductivity of post-perovskite in Earth's D″ layer. *Science*, **320**, 89–91.
Olsen, N., and Mandea, M., 2008. Rapidly changing flows in the Earth's core. *Nature Geoscience*, **1**, 390–394.
Roberts, P. H., and Aurnou, J. M., 2012. On the theory of core-mantle coupling. *Geophysical and Astrophysical Fluid Dynamics* (to appear).
Roberts, P. H., and Soward, A. M., 1972. Magnetohydrodynamics of the Earth's core. *Annual Review of Fluid Mechanics*, **4**, 117–154.
Roberts, P. H., Yu, Z. J., and Russell, C. T., 2007. On the 60-year signal from the core. *Geophysical and Astrophysical Fluid Dynamics*, **43**, 321–330.
Rogers, T. M., and Glatzmaier, G. A., 2006. Angular momentum transport by gravity waves in the solar interior. *Geophysical and Astrophysical Fluid Dynamics*, **653**, 756–764.
Schubert, G., Turcotte, D. L., and Olson, P., 2001. *Mantle Convection in the Earth and Planets*. Cambridge, UK: Cambridge University Press.
Sprague, M., Julien, K., Knobloch, E., and Werne, J., 2006. Numerical simulation of an asymptotically reduced system for rotationally constrained convection. *Journal of Fluid Mechanics*, **551**, 141–174.
Stellmach, S., and Hansen, U., 2004. Cartesian convection driven dynamos at low Ekman number. *Physical Review E*, **70**, 056312.

Stix, M., and Roberts, P. H., 1984. Time-dependent electromagnetic core-mantle coupling. *Physics of the Earth and Planetary Interiors*, **36**, 49–60.
Tanaka, S., 2010. Constraints on the core-mantle boundary topography from *P4KP-PcP* differential travel times. *Journal of Geophysical Research*, **115**, B04310, doi:10.1029/2009JB006563.
Taylor, J. B., 1963. The magnetohydrodynamics of a rotating fluid and the Earth's dynamo problem. *Proceedings. Royal Society of London*, **A274**, 274–283.
Tyler, R. H., 2008. Strong ocean tidal flow and heating on moons of the outer planets. *Nature*, **456**, 770–773.
Uno, H., Johnson, C. L., Anderson, B. J., Korth, H., and Solomon, S. C., 2009. Modeling Mercury's internal magnetic field with smooth inversions. *Earth and Planetary Science Letters*, **285**, 328–339.
Velicogna, I., and Wahr, J., 2006. Acceleration of Greenland ice mass loss in spring 2004. *Nature*, **443**, 329–331.
Vočadlo, I., Alfè, D., Price, G. D., and Gillan, M. J., 2000. First principles calculation of the diffusivity of FeS at experimentally accessible conditions. *Physics of the Earth and Planetary Interiors*, **120**, 145–152.
Wahr, J., and deVries, D., 1989. The possibility of lateral structure inside the core and its implications for nutation and Earth tide observations. *Geophysical Journal International*, **99**, 511–519.
Wahr, J., Swenson, S., and Velicogna, I., 2006. Accuracy of GRACE mass estimates. *Geophysical Research Letters*, **33**, L06401, doi:10.1029/2005GL025305.
Wicht, J., and Christensen, U. R., 2010. Torsional oscillations in dynamo simulations. *Geophysical Journal International*, **181**, 1367–1380.
Yoshida, S., Sumita, I., and Kumazawa, M., 1996. Growth model of the inner core coupled with outer core dynamics and the resulting elastic anisotropy. *Journal of Geophysical Research*, **101**, 28085–28103.
Yoshino, T., 2010. Laboratory electrical conductivity measurement of mantle minerals. *Surveys in Geophysics*, **31**, 163–206, doi:10.1007/s10712-009-9084-0.

Cross-references

Core Dynamo
Earth's Structure, Lower Mantle
Energy Budget of the Earth
Geomagnetic Field, Theory

CRUSTAL REFLECTIVITY (OCEANIC) AND MAGMA CHAMBER

Satish C. Singh
Laboratoire de Géoscience Marines, Institut de Physique du Globe de Paris, Paris, France

Synonyms

Melt lens; Spreading center and ridge

Definition

Axial magma chamber (*Melt lens*) is a thin melt lens observed at ocean spreading centers.
Layer 2A or *Lava* is the top layer of oceanic igneous crust.
Layer 2B is a dike sequence and lies above the axial melt lens.
Layer 3 (*gabbro*) forms the lower oceanic crust.
Moho is a boundary between the crust and mantle.
Pg is a seismic ray that travels through the crust.
PmP is a reflection from the crust–mantle boundary.
Pn is a ray that travels in the upper mantle.
Tomography is a technique to image the velocity structure of the earth.

Introduction

Over 70% of the earth's crust is formed by the cooling and crystallization of melt at ocean spreading centers, which represent over 55,000 km of chains of volcanoes in the middle of the oceans, called mid-ocean ridges. At ocean spreading centers, the oceanic plate separates causing the mantle to move upward, reducing the pressure and causing the melting of the mantle. Since the newly formed melt is lighter than the surrounding mantle material, it moves upward toward the surface of the earth. Part of the melt is erupted on the seafloor as lava, which cools very rapidly forming a cap of solid extrusive layer, also known as Layer 2A (Figure 1). As there is a significant amount of water present at mid-ocean ridges, the water circulates deep in the crust. Therefore, the melt stays mainly in the middle of the crust and erupts along thin dikes. When these dikes are cooled and crystallized, they form a thick intrusive layer or Layer 2B. Below the dikes, the melt could reside for a long period, forming a steady state melt lens, called axial melt lens or axial magma chamber (AMC). The magma cools and crystallizes in this melt lens, forming a crystalline lower crust. The melt lens forms the lower limit for further penetration of water, and therefore, partial melt is generally present beneath the melt lens down to the crust–mantle boundary. Sometimes hot melt ascending from the mantle may get injected in this partially molten region. Based on this basic process, the oceanic crust is divided into three layers, lava (extrusive), dikes (intrusive), and gabbroic crust. The relative

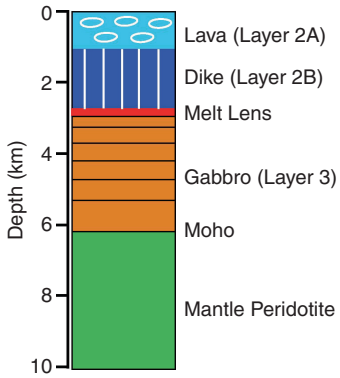

Crustal Reflectivity (Oceanic) and Magma Chamber, Figure 1 Classical model of the oceanic crust. Layers 2A and 2B form the upper crust whereas the gabbro layer corresponds to the lower crust.